Agent-based modelling of juvenile eel migration via selective tidal stream transport

Thomas Benson [a,*], Jasper de Bie [b], Jennifer Gaskell [c], Paolo Vezza [b], James R. Kerr [b], Darren Lumbroso [a], Markus R. Owen [c], Paul S. Kemp [b]

[a] HR Wallingford, Howbery Park, Wallingford, OX10 8BA, UK
[b] International Centre for Ecohydraulics Research, Faculty of Engineering and Physical Sciences, University of Southampton, Southampton, SO17 1BJ, UK
[c] School of Mathematical Sciences, University of Nottingham, Nottingham, NG7 2RD, UK

A B S T R A C T

Recruitment of temperate eel species *Anguilla anguilla, A. rostrata* & *A. japonica* has declined over the last few decades due to human activities, such as overfishing and construction of migratory barriers (e.g. dams, weirs and sluices) and hazardous energy infrastructure (e.g. turbines, intakes and outfalls). Numerical models, substantiated with data from field and laboratory studies, can potentially predict and quantify the relative impacts of such activities, thereby assisting in the sustainable management of eel populations. Here, we present an agent-based model (ABM) of juvenile eel migration up estuaries. The model includes relevant eel behaviours and environmental conditions that, according to the literature, influence upstream migration. Crucially, by assessing the local salinity gradient and relative flow direction, the modelled eels (agents) self-determine whether the tide is flooding or ebbing and orientate themselves for navigation, with no top-down instructions. This allows the agents to decide which particular behaviour to undertake as part of Selective Tidal Stream Transport (STST). The developed ABM is coupled to a hydrodynamic model of the Thames Estuary and the results substantiated by comparison against eel trap data. Combinations of the various STST behaviours are systematically tested and the influence they have on up-estuary migration is assessed in terms of relative energy expenditure. The parameterised model is then used predictively at Milford Haven Waterway to investigate potential impacts on the juvenile eel population due to entrainment in a power plant cooling water intake and outfall. Results from the Thames model case study indicate that including bed anchoring behaviour is essential for achieving a good comparison with the eel trap data and the choice of salinity detection threshold is also important. If daylight avoidance (diel) behaviour is not included, the most energy efficient migration is achieved using just two STST behaviours (ebb tide bed anchoring and upward migration during flood). With diel behaviour included, energy expenditure is greater, but some efficiency is regained by including all of the STST behaviours. For the Milford Haven case study, the model predicted a juvenile eel intake and outfall entrainment rate of 2.0% and 4.7%, respectively. It is concluded that the ABM is a valuable tool for assessing potential impacts on the recruitment of eels (extendable to other species) and could be used to assist in site-selection and low impact design of energy infrastructure in tidal environments.

1. Introduction

All anguillid eels have a catadromous life cycle in which the juveniles migrate from the ocean into rivers where they mature for several years and then return to the ocean as adult silver eels to spawn (Tesch, 2008). The focus of this study is the swimming behaviour of juvenile European eels (*Anguilla anguilla*) in the latter stages of their migration as they progress up macro-tidal[1] estuaries to reach freshwater environments. At this stage in their life cycle they are approximately 8–12 cm

in length and translucent, so referred to as glass eels, and become elvers when more pigmented. In this study, the term juvenile eel will be used to describe both of these stages and for brevity we will usually refer to them as simply eel hereafter (unless clarity is needed). Furthermore, numerically modelled eel individuals will generally be referred to as agents.

The International Union for Conservation of Nature (IUCN) has classified the status of the European eel as critically endangered. Their decline is thought to be due to various anthropogenic factors

---

* Corresponding author.
  E-mail address: t.benson@hrwallingford.com (T. Benson).
  [1] Where the tidal range is in excess of 4 m.

(Dekker, 2003; MacGregor et al., 2008; Arai, 2014), such as entrainment in power plant intakes and outfalls or impingement on screens (Piper et al., 2015), blockage due to poorly designed fish passes and weirs (Amaral et al., 2002; Russon et al., 2010; Calles et al., 2013; Vowles et al., 2015), population losses due to commercial fishing (ICES, 2014) and impacts on larval stages due to climate change (Knights, 2003; Bonhommeau et al., 2008).

In an attempt to re-establish the European eel populations, legislation has been passed whereby EU member states must identify suitable eel habitats and manage these in a manner that ensures sufficient escapement of adult eels to the sea (European Commission, 2007). To achieve this, annual data on recruitment and commercial or recreational catch data are required (ICES, 2017). Currently, recruitment estimates and trends are derived from local catch data annually across the western part of Europe (ICES, 2017) and this information can further be used to provide larger scale estimates of recruitment via empirical modelling (Briand et al., 2006; Bru et al., 2009).

Despite numerous studies into the topic of eel migration, current knowledge of how eels migrate from the continental shelf, through tidal estuaries and into freshwater environments is limited (Cresci, 2020). This is partly due to the difficulty of monitoring these small semi-transparent life-stages which tend to migrate during the night to avoid predation, often in turbid water (i.e. low underwater light transmission levels caused by suspended sediment). Most information on their migratory behaviour has, therefore, been obtained from controlled laboratory experiments and from catch data using fishing nets or eel traps located on weirs or sluices.

Laboratory studies have been used to determine the swimming speeds of juvenile European eel. (Vezza et al., 2020) recorded a sustained swim speed (20–200 min duration) of approximately 0.05 m s^{-1}, prolonged speeds (up to 20 min duration) of between 0.2 to 0.4 m s^{-1} (dependent on water temperature) and maximum burst speeds of up to about 0.5 m s^{-1}. Field studies have also shown that they are unable to progress upstream against currents greater than 0.36 to 0.50 m s^{-1} (Creutzberg, 1961; McCleave, 1980). Depth-averaged flow speeds in many estuaries often exceed 1 m s^{-1} during the outbound (ebb) tide. It is therefore necessary that the eels perform decision making and exhibit behavioural strategies that allow them to efficiently make headway to reach the tidal limit.

A conceptual model that describes how eels navigate up estuaries is called Selective Tidal Stream Transport (Harrison et al., 2014). In this model, eel individuals follow three key behavioural regimes in response to the time-varying state of the tide. First, during the inbound (flood) tide, the eels are assumed to drift with the flow to conserve energy and are dispersed throughout the water column. Second, after slack high water, during the early stages of the following outbound (ebb) tide, the eels are assumed to move towards the edges of the channel where the flows are slower, thus allowing them to continue progressing upstream. Third, as the ebb flows increase, the eels are assumed to swim to the bed and anchor themselves, thus preventing themselves from being carried back downstream.

One way of quantitatively assessing the advantages or disadvantages of STST behaviour, for example in terms of energy expenditure, is to use a numerical model. Key variables, such as swim speed, can be easily manipulated in a numerical model and assessed in terms of relative sensitivity on the outcomes. Furthermore, a wide variety of conditions can be tested. Numerical models can also help to bridge gaps in understanding between data collected from field or laboratory studies (Grimm and Railsback, 2005). Field data, such as from net catches or eel traps, are crucial for supporting a model or theory but are often sparse or incomplete in both time and space. On the other hand, data sets from small scale laboratory studies are useful for isolating and quantifying behaviours in a controlled manner (e.g. swim speed, light sensitivity, or rheotaxis[2]) making them suitable for gathering model calibration data. However, laboratory experiments cannot incorporate all of the complexity of the physical estuarine environment, such as tidal flows, river discharge, turbidity, daylight, salinity, and temperature, which all affect eel behaviour to some degree (Cresci, 2020) and vary continuously in space and time. Combining the three disciplines (i.e. numerical models, *in situ* data collection and controlled laboratory experiments) is therefore crucial for gaining a better understanding of the migratory behaviour of eels (and indeed other fish species).

One form of numerical model that is suitable for simulating fish dynamics and behaviour is an agent-based model (ABMs). Within an ABM, a collection of autonomous decision-making entities called agents are represented and each agent individually assesses its situation and makes decisions on the basis of a set of rules (Bonabeau, 2002). This approach can be applied to simulating the movements and decision-making of fish in which individuals use relatively simple behavioural rules that are dependent on their surrounding environment (Jager and DeAngelis, 2018). ABMs have been applied successfully in ecological research and are a valuable tool in predicting fish recruitment (DeAngelis and Mooij, 2005; McLane et al., 2011). For example, past modelling studies have reproduced annual trends and estimates for species such as Atlantic cod *Gadus morhua* and European anchovy *Engraulis encrasicolus* (Daewel et al., 2015; Ospina-Alvarez et al., 2015). ABMs of fish behaviour have also been used successfully at smaller temporal and spatial scales. For example, (Goodwin et al., 2006) developed an ABM using a Eulerian–Lagrangian-Agent Method (ELAM) to mimic the swimming behaviour of fish around man-made structures such as fish passes and weirs.

In the present study, an ABM is developed for simulating the upstream migration of European eel through macro-tidal estuaries. Behavioural rules and abilities of the eels are defined based on an earlier assessment of the literature on this subject (Cresci, 2020). Parameterisation and testing of the model is performed using two case studies. In the first case study, the ABM is coupled to a three-dimensional hydrodynamic model of the Thames Estuary (UK). The aim of this case study is to assess the relative importance of the various STST behaviours on migration efficiency and to verify the model results against eel trap data collected at Stoney Sluice in Brentford, where the River Brent joins the tidal Thames. In the second case study, the parameterised ABM is applied to the Milford Haven Waterway estuarine environment and used to predict entrainment of eels in the cooling water intake and outfall of Pembroke Power Station.

2. Agent-based model description

This section describes the ABM which consists of a particle tracking model and an eel behaviour model. User specified parameter values for the described formulae vary according to calibration and are given in the subsequent case study sections.

2.1. Particle tracking model

The general approach of the ABM is to simulate agents (in this case eels) as a set of discrete points (Lagrangian framework) which move within, and are influenced by, the three-dimensional flow field provided by a gridded hydrodynamic model (Eulerian framework). The underlying model for performing the Lagrangian calculations (without eel behaviour) is called HydroBoids, which was developed previously at HR Wallingford for modelling dispersion of fish larvae (Wallingford, 2016), behaviour of fish species in response to stimuli such as underwater noise (Benson et al., 2016) and assessing collisions of marine species with tidal turbines (Rossington and Benson, 2020). The model, which is coded in the Matlab programming environment (www.mathworks.com), was further developed during the current work to include the behaviour of juvenile eel migration up estuaries (described in Section 2.2).

---

[2] The movement of an organism towards or away from an oncoming current of water.

HydroBoids requires as input the 3D flow vector field from a Eulerian grid hydrodynamic model and then performs the necessary time and space interpolation for obtaining the velocity vector at the centre of each modelled agent. Using this information, the cumulative displacement (dx, dy, dz) of each agent, located at $\mathbf{x} = (x, y, z)$, is tracked at discrete time intervals (dt) using a standard particle tracking formula (Monti and Leuzzi, 2010) with an additional term for the agent swim velocity components, written as:

$$\begin{pmatrix} dx(t) \\ dy(t) \\ dz(t) \end{pmatrix} = \left[\begin{pmatrix} U(\mathbf{x},t) \\ V(\mathbf{x},t) \\ W(\mathbf{x},t) \end{pmatrix} + \begin{pmatrix} U_a(t) \\ V_a(t) \\ W_a(t) \end{pmatrix} + \begin{pmatrix} \sqrt{2K_x} & 0 & 0 \\ 0 & \sqrt{2K_y} & 0 \\ 0 & 0 & \sqrt{2K_z} \end{pmatrix} \begin{pmatrix} \gamma_x \\ \gamma_y \\ \gamma_z \end{pmatrix} \right] dt \quad (1)$$

For each agent, the resultant path travelled is a function of the 3D flow velocity vector (U, V, W), the agent's swim vector (U_a, V_a, W_a), and turbulent diffusion, which is calculated using the diagonal components of the Eulerian eddy diffusivity tensor (K_x, K_y, K_z) and independent random numbers $(\gamma_x, \gamma_y, \gamma_z)$ for each axis selected from a normal distribution with mean of zero and variance of one $(\mathcal{N}(0,1))$.

The vertical component of the eddy diffusivity in Eq. (1) varies with height (z) above the bed and is modelled using a mixing length model (Prandtl, 1925) as a function of the bed shear velocity (u_*), water depth (h), and a characteristic mixing length $(\kappa = 0.41)$, as:

$$K_z(z) = \beta \kappa u_* z \left(1 - \frac{z}{h} \right) \quad (2)$$

The bed shear velocity in Eq. (2) is in turn dependent on the flow speed, water depth and bed friction (z_0), as:

$$u_* = \frac{\kappa U(z)}{\ln\left(\frac{z}{z_0}\right)} \quad (3)$$

Bed friction is prescribed in the model using a Nikuradse roughness length which is related to z_0 as $k_s = 30z_0$ (Nikuradse, 1933); β is the Prandtl number, with a value between 0 and 1, to reduce the turbulent displacement since fish will disperse less quickly than the water. For the horizontal diffusion $(K_x$ and $K_y)$, a constant eddy diffusivity coefficient is applied everywhere in both the x and y directions.

At a specified time step interval, the 3D positions of all the tracked agents are saved to binary results files for subsequent post-processing. Information on the swim speed, heading and elevation angle of the agents is also recorded in the file to allow 3D visualisation of the their movements.

2.2. Eel behaviour model

The ABM of upstream migrating eels was developed during this study using the three STST regimes of behaviour which occur at different stages of the tidal cycle (flood, ebb and early ebb tide). Importantly, the modelled eels, or agents, are assumed to be able to determine the tidal state and hence which regime they are in by assessing the local salinity gradient and flow velocity field. They are therefore self-governing agents without any external (top-down) instructions on their movement. The dynamics of the model are described below and represented as a flowchart in Fig. 1.

2.2.1. Initialisation

At the start of the simulation, $t = 0$, eel agents are placed into the flow model domain as discrete points in 3D space (x, y, z) within a user defined region. The swim speed of each agent (v_{swim}) is randomly selected from a Gaussian distribution of speeds with a specified mean $(\bar{v}_{swim})$ and standard deviation (σ_{swim}), obtained from laboratory experiments performed over a range of temperatures, to represent the variability in the population (Vezza et al., 2020). The swim speed for each agent remains constant throughout a simulation except for when they temporarily anchor themselves at the bed (Section 2.2.4) or drift during the flood tide (Section 2.2.5). The initial heading (θ_{swim}) of each agent is also randomly selected between 0 and 360°, and the elevation angles (ϕ_{swim}) are initialised to zero. The behavioural rules then bias subsequent swim angles according to the salinity and tide.

2.2.2. Position updating and land avoidance

Before the new agent position is calculated using Eq. (1), additional random variability in the agent navigation (other than turbulence), is applied by adding a small angular error, or *persistence angle*, in radians to both the agent's heading (θ_{swim}) and vertical elevation angle (ϕ_{swim}) at each time step (Eq. (4) and (5)). The persistence angle is selected from a normal distribution, which has a mean of zero and separate standard deviations for the horizontal and vertical $(\sigma_h$ and $\sigma_v)$, then added to the heading and elevation angle of the fish in the polar coordinate system. In general, a smaller standard deviation for vertical persistence (σ_v) is used since fish tend to navigate more in the horizontal direction.

$$\theta_{swim} = \theta_{swim} + \mathcal{N}(0, \sigma_h^2) \quad (4)$$

$$\phi_{swim} = \phi_{swim} + \mathcal{N}(0, \sigma_v^2) \quad (5)$$

Because the persistence angle is applied to the agent's heading, the magnitude of the resultant navigation error at each time step is dependent on the swim speed of the agent, becoming zero if the swim speed is zero (i.e. drifting). Vertical turbulent eddy viscosity (K_z) on the other hand varies according to flow speed and depth, becoming zero in still water. It is therefore important to model random displacement due to both persistence error and turbulent diffusion.

Using the set of agent swim speeds (v_{swim}), modified headings (θ_{swim}) and elevation angles (ϕ_{swim}) from either the initialisation step or the end of the previous time step, in addition to the interpolated flow vectors (v_{flow}), the agents are moved to their new positions according to Eq. (1) (see Section 2.1).

The moved agents can occasionally encounter land either by crossing a model land boundary or by entering dry areas (with zero water depth) such as tidal flats. In such instances, to simulate active avoidance behaviour by an agent, an iterative process occurs in the model whereby the agent modifies its previous trajectory heading by 10 degree increments (simultaneously both left and right of its current heading) and tests to see if the new position is within water. The first non-dry position is kept and the iterations are finished. If the heading increments reach 180 degrees, then the agent is assumed to be stranded on a dry model element and its original position at the beginning of the time step is kept. Stranded agents are assumed to survive in the model and they reattempt navigation during each subsequent model iteration. This allows the agents to be re-entrained into the water column on a following high tide.

2.2.3. Assessment of tidal state

At the beginning of each time step, the eel agents assess the surrounding salinity gradients interpolated from the hydrodynamic model at their body centres. For each agent, if the salinity is detectable $(S > S_{thresh})$ and there is also a discernible horizontal salinity gradient $(|\nabla S| > \nabla S_{thresh})$, the agent actively aligns itself with the flow vectors. Refer to Section 3.4.2 for threshold values. The direction of alignment (with or against the flow vector) is chosen to be that closest to the direction of decreasing salinity $(\theta_{-\nabla S})$, and in doing so it is assumed to be pointing up the estuary. The direction of the flow vector relative to the agent's heading consequently determines whether the agent detects an ebbing or flooding tide, and hence determines which behaviour the agent will perform during this model time interval (Fig. 1).

If an agent enters a freshwater region, or a region where there is no salinity gradient, then it is assumed to have no directional cue to follow. In this case, it continues in the same direction as the previous time interval using a correlated random walk (Eq. (4) and (5)). The agent might therefore continue up the estuary, even if there are meanders, by encountering the banks and consequently following the channel alignment. There is also a chance that it will turn around due to the random walk, or it may become trapped in an embayment until the salinity returns to higher levels on a subsequent flood tide.
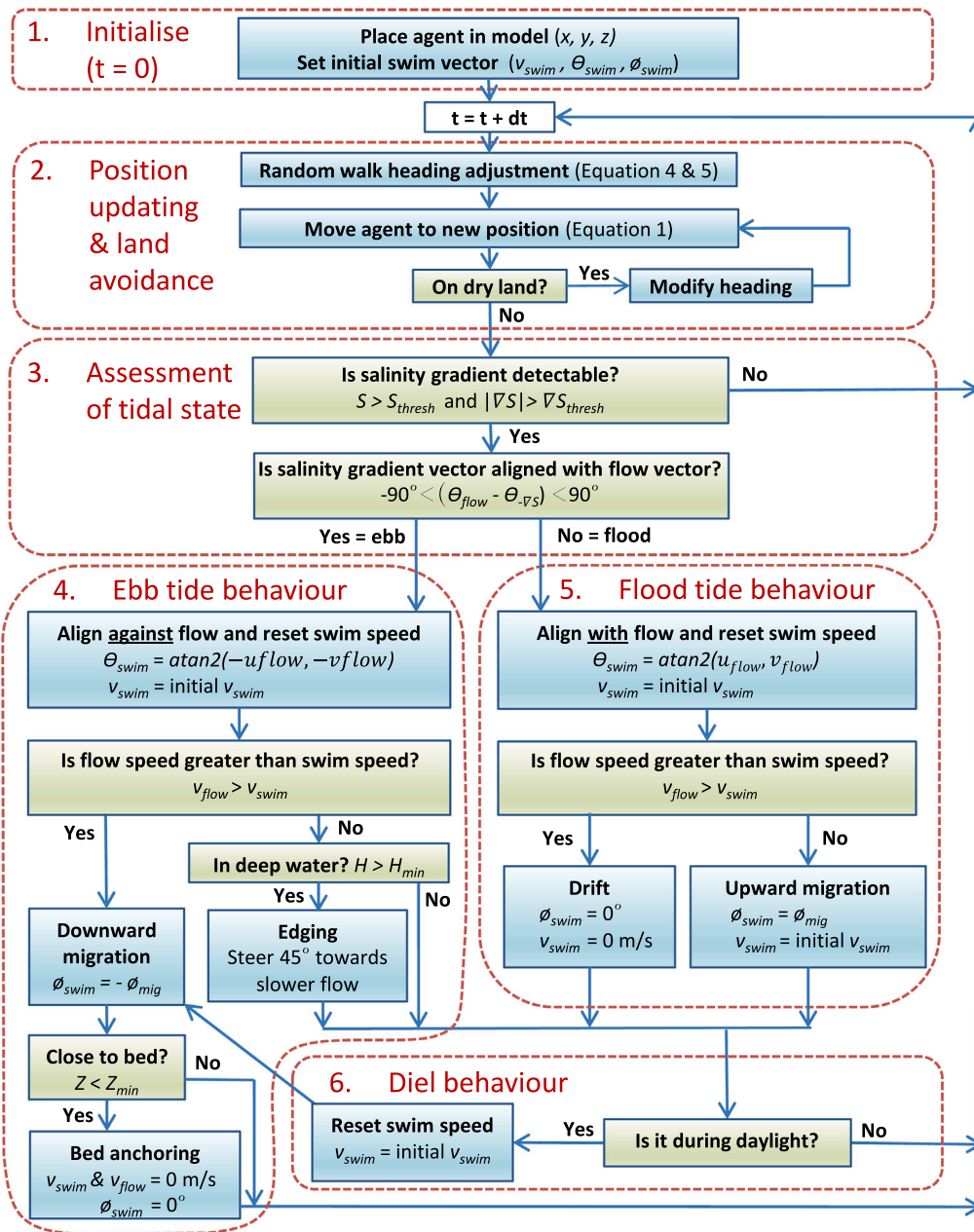
1. Initialise (t = 0)

Place agent in model (x, y, z)
Set initial swim vector $(v_{swim}, \Theta_{swim}, \varnothing_{swim})$

$t = t + dt$

2. Position updating & land avoidance

Random walk heading adjustment (Equation 4 & 5)

Move agent to new position (Equation 1)

On dry land? — Yes → **Modify heading**

No

3. Assessment of tidal state

Is salinity gradient detectable?
$S > S_{thresh}$ and $|\nabla S| > \nabla S_{thresh}$ — No

Yes

Is salinity gradient vector aligned with flow vector?
$-90^\circ < (\Theta_{flow} - \Theta_{-\nabla S}) < 90^\circ$

Yes = ebb   No = flood

4. Ebb tide behaviour

Align against flow and reset swim speed
$\Theta_{swim} = atan2(-uflow, -vflow)$
$v_{swim} = $ initial v_{swim}

Is flow speed greater than swim speed?
$v_{flow} > v_{swim}$

Yes   No

In deep water? $H > H_{min}$

Yes   No

Downward migration
$\varnothing_{swim} = -\varnothing_{mig}$

Edging
Steer 45° towards slower flow

Close to bed?
$Z < Z_{min}$ — No

Yes

Bed anchoring
v_{swim} & $v_{flow} = 0$ m/s
$\varnothing_{swim} = 0^\circ$

5. Flood tide behaviour

Align with flow and reset swim speed
$\Theta_{swim} = atan2(u_{flow}, v_{flow})$
$v_{swim} = $ initial v_{swim}

Is flow speed greater than swim speed?
$v_{flow} > v_{swim}$

Yes   No

Drift
$\varnothing_{swim} = 0^\circ$
$v_{swim} = 0$ m/s

Upward migration
$\varnothing_{swim} = \varnothing_{mig}$
$v_{swim} = $ initial v_{swim}

6. Diel behaviour

Reset swim speed
$v_{swim} = $ initial v_{swim} — Yes — **Is it during daylight?** — No

Fig. 1. Flow diagram of upstream migration of juvenile eels, navigating in the direction of decreasing salinity gradient. The six boxes (dashed lines) correspond to the descriptions presented in Sections 2.2.1–2.2.6 respectively.

2.2.4. Ebb tide behaviour

When an agent detects that it is an ebb tide, if the local flow speed is less than the agent's initialised swim speed ($v_{flow} < v_{swim}$), initiation of so-called *edging* behaviour occurs (Fig. 1). Edging is most likely to occur close to either high or low water during the early or late ebb, but its effect will be greatest during early ebb because of the higher tidal level at this time and hence wider channel cross-section. A minimum threshold on local water depth (H_{min}) is used to prevent agents from swimming into very shallow water and getting stuck on intertidal areas. If either the flow speed or minimum depth criteria are not met, edging behaviour is not initiated. When activated, each affected agent moves towards the channel boundaries, whilst also swimming against the flow. This is achieved by adjusting the heading of the agent by 45° from its present flow-aligned heading towards decreasing flows.

During stronger ebb tide flows, when by default an agent will be heading into the flow (± 45°), if the oncoming current speed exceeds

its swim speed ($v_{flow} > v_{swim}$) (Fig. 1) then it actively migrates down to the bed at a user specified elevation angle (ϕ_{mig}). When within a small distance of the bed (Z_{min}), the agent is assumed to hold itself stationary on the substrate, referred to as *bed anchoring* behaviour. As soon as the agent is able to make headway against the flow $v_{flow} <= v_{swim}$ this behaviour ceases and the agent's speed is returned to its initial speed. Upwards migration or drifting is then initiated as described in the following section.

2.2.5. Flood tide behaviour

When an agent detects that it is a flood tide, if the flow speed is less than the agent's initial swim speed then it swims upwards towards the surface at a user specified elevation angle (ϕ_{mig}). If the flow speed is faster, then the agent's swim speed is set to zero to simulate drifting behaviour (Fig. 1) thus saving energy during upstream movement. During drifting behaviour, the eel agents are treated as
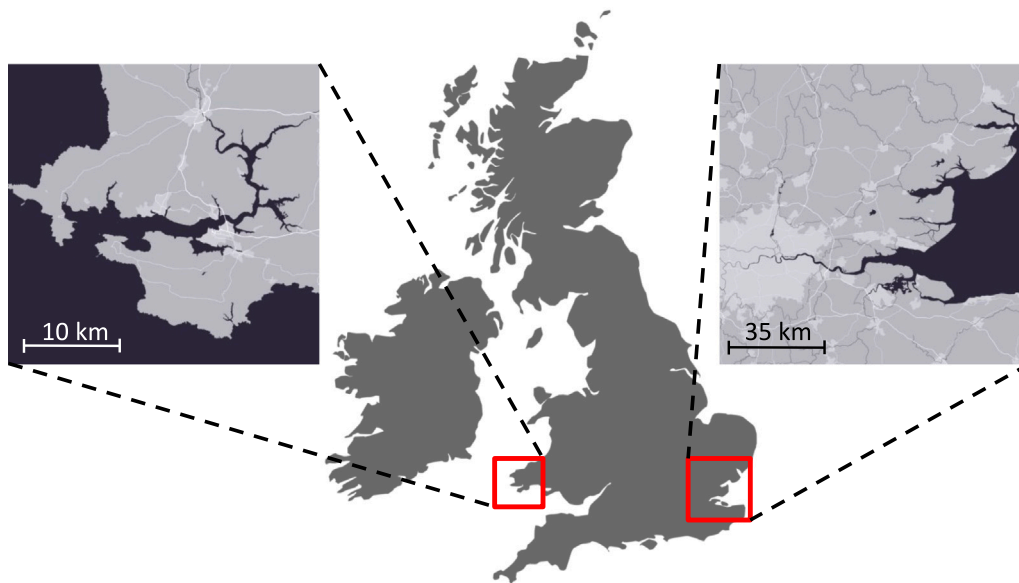
Fig. 2. Location of the two estuaries in the UK used for parameterisation and application of the ABM. *Right*: Thames Estuary (Case study 1). *Left*: Milford Haven Waterway (Case study 2); Zoomed portions of the map are to different scales.

passive Lagrangian particles which are advected and dispersed solely by the 3D modelled currents and turbulence.

2.2.6. Diel behaviour

Previous field studies have reported that juvenile eels avoid daylight, presumably as an anti-predatory behaviour, and migrate mainly during hours of darkness (De Casamajor et al., 1999). During daylight hours they stay hidden in the deeper parts of the water column and halt their movements. To simulate this diel behaviour, the time of day is assessed in the model at each time interval. Between sunrise and sunset it is assumed the agents are able to detect the sunlight and are programmed to swim to the bed then anchor themselves as described in Section 2.2.4. This behaviour is not strictly part of the STST set of behaviours but was included in the model in order to investigate the cost in terms of relative energy expenditure due to this known anti-predatory behaviour.

3. Case study 1: Modelling juvenile eel migration in the Thames estuary

3.1. Overview

This case study assesses the relative importance of the various STST behaviours for eel migration. The model results are also verified against eel trap data collected at Stoney Sluice in Brentford Creek (a tributary to the tidal Thames).

3.2. Site description

The Thames is the second longest river in the United Kingdom, ranging over 346 km from its source in Gloucestershire to the estuary, which passes through central London and continues to its mouth at Southend-on-Sea (Essex) where it drains into the North Sea. The Thames River Basin District (RBD) covers and area of approximately 16,000 km^2 including the Greater London area and parts of Oxfordshire and Kent (DEFRA, 2010) (Fig. 2). The tidal limit is at Teddington Lock, approximately 112 km from the mouth.

3.3. Observations of juvenile eels in the thames

Historically, the river supported eel fisheries but the population severely declined due to anthropogenic actions, e.g. water pollution in the 1980s, and flood defence engineering and barrier construction (Naismith and Knights, 1988; DEFRA, 2010). Monitoring of juvenile eel migration has intermittently been conducted in the past. Between 1985 and 1987, traps were installed at locations near the estuary tidal limit and further upstream and around 9000 individuals were caught, mostly glass eels (Naismith and Knights, 1988). Between 2005 and 2009, three tributaries (Rivers Roding, Darent and Mole) were sampled with similar traps and a decrease in recruitment of 99% was reported (Gollock et al., 2011). Since 2011, the Zoological Society of London (ZSL) and the Environment Agency has been involved in monitoring of numbers of migrating juvenile eels in the Thames RBD at several monitoring sites (EWCP, 2017). The 2014 trap data for one of the sites, Stoney Sluice in Brentford (Lat: 51.48424, Lon: −0.30957), has been used here to parameterise the ABM. Stoney Sluice is at the junction between the River Brent and Brentford Creek which adjoins the tidal Thames.

The 2014 Stoney Sluice eel trap data (Fig. 3) show that eels mainly started passing the sluice in early July and there was a general increase in trapped numbers throughout the measurement period (to the end of September). The time series consists of a number of peaks separated by periods of a few days (up to about 10 days) when the number of trapped eels decreased by an order of magnitude. According to the survey logs, the traps continued to work well during most of the measurement period, thus discounting this as the cause of the variability. However, there is a two week period (August 13th to 26th) during which no eel trap data were recorded due to pump failure (Fig. 3).

Eels started to arrive during a period of very low run-off and the peaks appear to coincide with short-term increases in run-off, presumably due to rain events (Fig. 3A). However, it is not clear from this visual comparison how river discharge could explain all of the peaks and troughs in the eel count data.

Another possible cause of the temporal variability in eel counts is temperature. Field experiments conducted by various researchers in estuaries other than the Thames have found a link between temperature and the onset of migration (Gascuel, 1986; Moriarty, 1986; White and Knights, 1997a,b), migration peak (White and Knights, 1997a) and the number of migrants (Hvidsten, 1985; Vøllestad and Jonsson, 1988). In
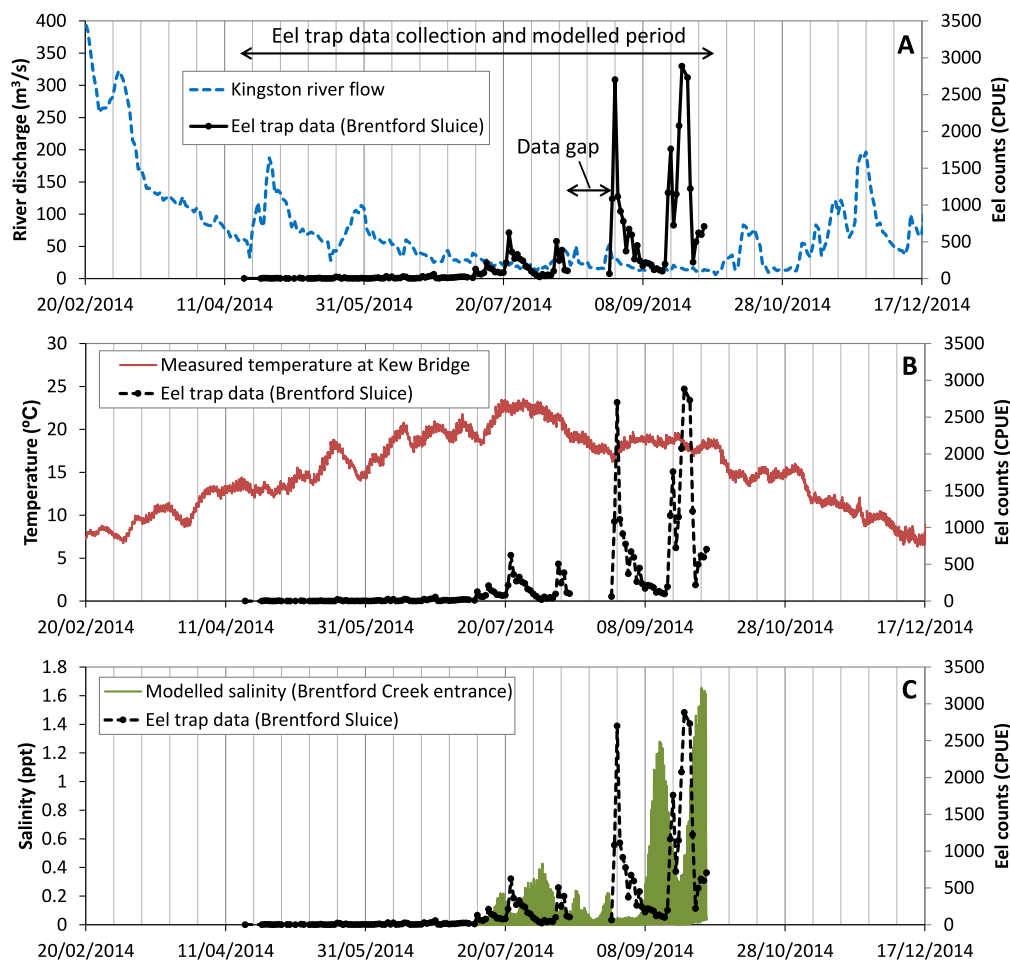
Fig. 3. Eel trap data at Stoney Sluice (2014) compared with: (a) River discharge recorded at Kingston (approximately 2 km upstream from Teddington Lock); (b) Measured temperature at Kew Bridge, approximately 1 km from Brentford Creek entrance, and (c) Modelled salinity at Brentford Creek entrance.

general, the minimum threshold for migration up estuaries to occur has been reported to be between 10–14 °C, with increased migration above 14–16 °C and peaking at 18–20 °C (White and Knights, 1997a,b; Moriarty, 1986; Naismith and Knights, 1988). For the present study, water temperature data were available at a recording station at Kew, approximately 1 km from the entrance to Brentford Creek (Fig. 3B). Water temperature was greater than 14 °C for the whole data period. Hence temperature is unlikely to be a limiting factor on migration during this period. The low numbers of eels trapped during the first three months suggests that another factor must be impeding their migration.

A better indication of the cause of the time variability can be seen by comparing the trapped eel counts with the modelled salinity at Brentford Creek (Fig. 3C) which shows an inverse relationship, but only following periods when there were detectable levels of salinity. Possible reasons for this relationship will be considered in the discussion.

3.4. Methods

3.4.1. Hydrodynamic model description

To provide the flow environment for the ABM, a 3D numerical model of the Thames estuary between Teddington Lock and Southend Pier (Fig. 4) was constructed using the TELEMAC-MASCARET modelling suite (TELEMAC-MASCARET Consortium). Tidal flows and salinity distribution were simulated for the five month period (April to September) during 2014 for which eel trap data were available.

The horizontal resolution of the unstructured triangular model mesh was in the range 5 to 500 m, with the finer resolution in the narrower

upstream sections and around small islands and bridge piers. The piers for all of the Thames bridges and the tidal barrage at Woolwich were included in the model. The vertical discretisation of the model consisted of four planes, with one at both the bed and surface, and the other two spaced at 10% and 50% of the water column height above the bed. This vertical discretisation has been found to be sufficient for accurately modelling the hydrodynamics and salinity within the Thames (Wallingford, 2018), which is mainly well mixed in the vertical.

The tidal boundary of the model at Southend Pier was driven using harmonically synthesised tides for the modelled period. No atmospheric surge component was included in the simulated water levels. At the upstream boundary of the model at Teddington, a time-varying river discharge was applied using daily gauge data for Kingston Lock (sourced from the Environment Agency).

At Richmond, approximately 5 km downstream from Teddington, a half tide weir was installed in 1894. The weir is raised during the lower half of each tide to ensure sufficient navigable depth in the channel upstream of the weir between Richmond and Teddington. The weir was included in the model by dynamically raising the bed elevation across the estuary at the weir location when the water level dropped below 1.72 m above Ordance Datum (Newlyn) and lowering it again when the downstream levels returned to higher values on the following flood tide.

3.4.2. Eel swim speed and dispersion parameterisation

Values for each of the input parameters for the eel behaviour model (as described in Section 2.1) are shown in Table 1. Swimming
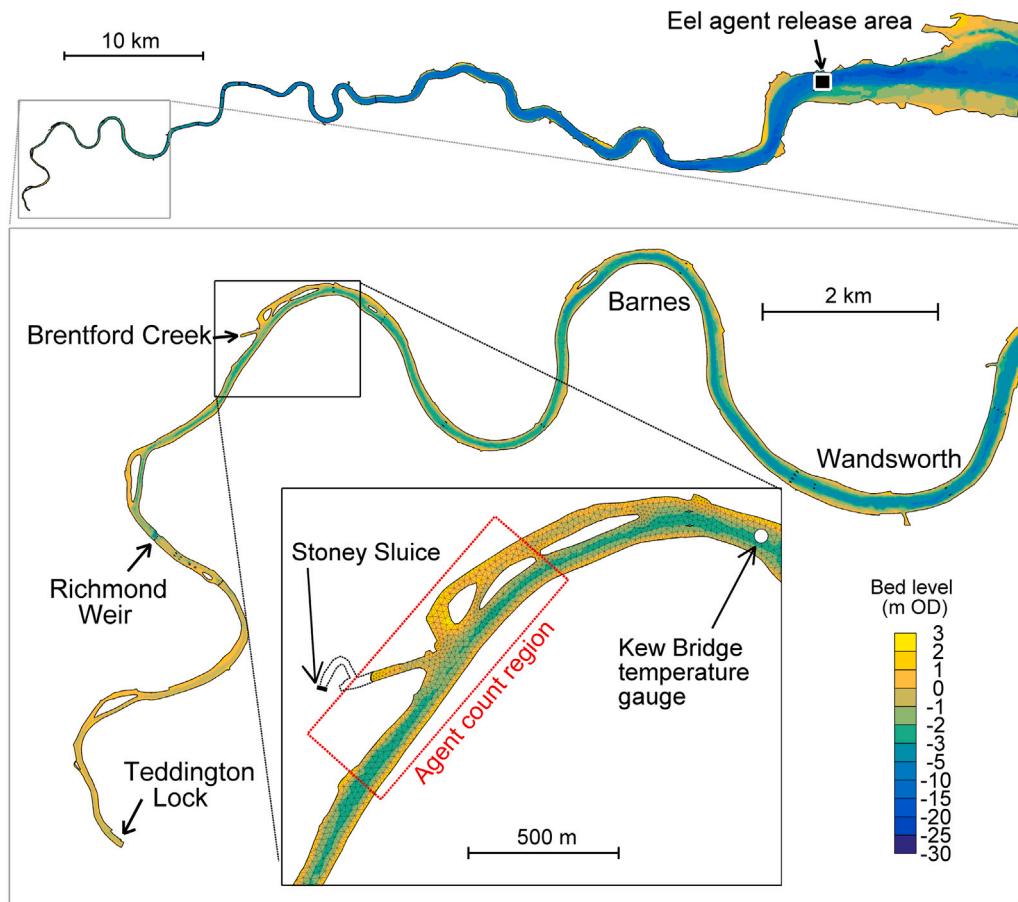
Fig. 4. Thames estuary model mesh and bathymetry showing the agent release area and detail of the upper reaches and Brentford Creek.

speed was derived from laboratory experiments performed by (Vezza et al., 2020), who studied the swimming capabilities of glass eels at water temperatures ranging from 8–18 °C, which is consistent with the temperature range recorded during the eel trap measurements (Fig. 3B). Prolonged (1–20 min) and sustained (20–200 min) swimming speeds were reported as 0.35 and 0.04 m s^{-1}, respectively. The long-term average speed of the eels is likely to be between these two values and the precise value is dependent on how long it takes for the eels to recover from prolonged swimming.

In the absence of any information on juvenile eel recovery time in the literature, an average swimming speed of 0.20 m s^{-1} was chosen which was applied in all the model scenarios except one (Scenario 10). The speed of each eel agent was prescribed randomly from a Gaussian distribution with a mean speed of 0.20 m s^{-1} and standard deviation of 0.05 m s^{-1}. Sensitivity to swim speed was assessed separately in Scenario 10 (see Section 3.4.4) in which the mean speed of the agents was set to 0.35 m s^{-1}, equal to the reported prolonged speed of glass eels. Neither interaction between agents nor time-varying temperature dependence on their swim speed was included in the model.

Random error in the eel agent navigation was prescribed with a horizontal and vertical standard deviation of 5° and 0°, respectively (Eqs. (4) and (5)).

To include the effect of turbulence on movement (important if the agents were drifting in the model), the vertical diffusivity was calculated using Eq. (2) and the Prandtl number was set to 0.5. Bed friction in the model was assumed to be equal to a Nikuradse roughness length of 0.01 m everywhere which is a typical value used for bed sediment composed of mixtures of mud, sand and gravel (Soulsby, 1990). For horizontal dispersion of the eel agents Eq. (1), a constant eddy viscosity coefficient of 0.1 m^2·s^{-1} was applied, which is a typical value for estuaries (Fischer et al., 1979).

Table 1

Parameter values used in the agent-based model of juvenile eel migration, for both case studies.

Parameter name	Symbol	Value
Temporal resolution:		
Time step	dt	30 s
Swim speed and persistence:		
Average swim speed	$\bar{v}_{swim}$	0.2 m s^{-1}
Swim speed standard deviation	σ_{swim}	0.05 m s^{-1}
Horizontal persistence error	σ_h	5°
Vertical persistence error	σ_v	0°
Turbulent dispersion:		
Horizontal eddy diffusivity	K_x, K_y	0.1 m^2 s^{-1}
Hydraulic bed roughness	k_s	0.01 m
Prandtl number	β	0.5
Navigation:		
Salinity detection threshold	S_{thresh}	0.04 ppt
Salinity gradient detection threshold	∇S_{thresh}	10^{-7} ppt m^{-1}
Minimum depth for edging behaviour	H_{min}	2 m
Vertical migration swim angle	ϕ_{mig}	70°
Distance from bed to start anchoring	Z_{min}	0.1 m

3.4.3. Salinity detection threshold calibration

The choice of threshold for the detection of salinity (S_{thresh}) was found to be an important calibration parameter for predicting the temporal trends observed in the eel trap catch data (Fig. 3). A suitable value for salinity threshold was determined iteratively by running the ABM several times for a range of different values and calculating the number of eels within 500 m distance of the entrance to Brentford Creek for comparison with the eel trap data. In these tests, the eel agents were programmed to perform all the STST behaviours, but with

Table 2
STST behaviour scenarios used in simulating eel upstream migration through the Thames Estuary.

Scenario	Swim down and anchor during ebb	Anchor during daylight	Upward migration on flood[c]	Edging during slow ebb[b]	Drifting during fast flood[b]
1					
2	✓	✓			
3	✓	✓	✓		
4	✓		✓		
5	✓	✓			✓
6	✓	✓	✓	✓	
7	✓	✓	✓	✓	✓
8	✓		✓	✓	
9	✓		✓	✓	✓
10[a]	✓	✓	✓	✓	

[a] Same as Scenario 6 but with faster eel swim speed.
[b] Fast flows were considered to be those greater than the eel agents swim speed.
[c] Without upward migration, the eel agents had no preference on swim height.

no diel behaviour (i.e. the same as Scenario 9 in the STST sensitivity tests described in the following section).

An approximate estimate of the threshold value was first obtained by a visual comparison of the time series of salinity and trapped eel numbers at the mouth of Brentford Creek (Fig. 3C). At times when significant numbers of eels were trapped, the modelled salinity at the entrance to the creek was generally less than 0.1 ppt. Assuming that this represented the approximate limit of the eel sensitivity to salinity, three ABM simulations were run using thresholds of 0.02, 0.04 and 0.08 ppt from which a more precise threshold value could be determined.

The choice of salinity gradient threshold (∇S_{thresh}) was found to be less important than the salinity detection threshold (S_{thresh}) because, in general, the salinity in the Thames estuary model showed strong gradients in places where the salinity was above the absolute salinity threshold. It was therefore set to a value close to, but slightly greater than, zero to ensure a sensible directional cue was provided to the eels for navigation. The chosen value for ∇S_{thresh} used in all simulations was 10^{-7} ppt m^{-1}.

3.4.4. STST behaviour scenario testing

To understand the relative importance of each of the STST behaviours described in Section 2.2, a set of ten scenarios were simulated, each with various parts of the behaviour switched off (Table 2).

Scenario 1 investigated the eel migration under the assumption of no STST behaviour other than navigation by detection of the salinity gradient. The rest of the scenarios were chosen to evaluate the relative efficiency saving of each key behaviour compared to continuous active upstream swimming. The first STST behaviour under investigation was downward migration and bed anchoring during the ebb tide. Because of its importance in migration, this was switched on for all of the STST scenarios (other than Scenario 1). In most of the scenarios, bed anchoring also occurred during daylight hours (i.e. diel behaviour), but this behaviour was switched off in three scenarios (4, 8 and 9) to test its effect on migration. Also for most of the tests, the eel agents were programmed to perform upward migration, swimming to the surface during the flood tide where the flow was faster. This behaviour was turned off in Scenarios 2 and 5 in which case the eels were assumed to have no preference on height. Three of the scenarios (5, 7 and 9) also investigated the effect of passive drifting rather than active swimming during the flood phase of the tide. The last five scenarios included edging behaviour to assess its importance on migration. The final scenario (10) used the same settings as Scenario 6, but with a faster average swim speed of 0.35 m s^{-1}.

At the start of each model scenario, eel agents were placed at a height of 0.1 m from the seabed in a 1.2 km square grid with a spacing of 5 m in the main channel close to the London Gateway port, approximately 14 km from the seaward boundary at Southend Pier (Fig. 4). Those initialised in water depths less than 0.1 m were removed

since they were deemed to be stuck on intertidal areas (i.e. mudflats), resulting in a total of 58,057 placed agents.

All the model scenarios were run for the same five month (165 days) period commencing at midnight on 18th April 2014 (when data collection began at Brentford) with a computational time step of 30 s. Throughout each simulation, batches of 24 agents were randomly selected every 2 h to be released from the start grid, thus totalling 47,520 released. The position order of the randomly selected agents was made to be the same for each modelled scenario by seeding the random number generator to a pre-saved state at the start of each simulation.

The model output files recorded the agent positions, swim speeds and heading at a sample interval of 15 min. On completion of each simulation, the files were post-processed to determine the numbers of agents within a distance of 500 m of the entrance to Brentford Creek. For assessing the efficiency of migration, the model scenario data were further processed to determine information on the average through-water distance swum, the total migration time and the percentage of released agents arriving by the end of the simulation. Assuming the eels were inactive when their modelled swim speed was zero (i.e. during bed anchoring or drifting), the total migration time was further split into the average period of time that the agents were either actively swimming (T_{active}) or inactive ($T_{inactive}$). Using these times, an estimate of the relative energy expenditure (E_{rel}) of migration was calculated for each model scenario according to the following equation.

$$E_{rel} = \frac{MR_{ratio}.T_{active} + T_{inactive}}{MR_{ratio}.T_{reference}} \qquad (6)$$

In Eq. (6), the reference time ($T_{reference}$) is the average active migration time for the constant swimming scenario. The calculation also requires an approximate value for the ratio (MR_{ratio}) between active metabolic rate (AMR) and inactive (or standard) metabolic rate (SMR). No measurements of these parameters were found in the literature for juvenile eels. However, a previous study using 3 year old hatchery *Anguilla anguilla* determined that the oxygen consumption rate (a proxy for metabolic rate) during swimming was approximately twice that during resting (van Ginneken et al., 2005). Assuming this ratio is the same for juvenile eels, a value of $MR_{ratio} = 2$ was used.

3.5. Results

3.5.1. Spatiotemporal patterns of migration up the estuary

Differences in spatiotemporal patterns between scenarios were generally small (Fig. 5). In all scenarios, the agents tended to congregate at the position of the contour of the salinity detection threshold (S_{thresh} = 0.04 ppt), generally located between about 0 and 40 km from Teddington. The first subplot in Fig. 5 shows the results for Scenario 1 (constant swimming). In this scenario, the agents were relatively dispersed spatially compared to the other scenarios due to fact that the
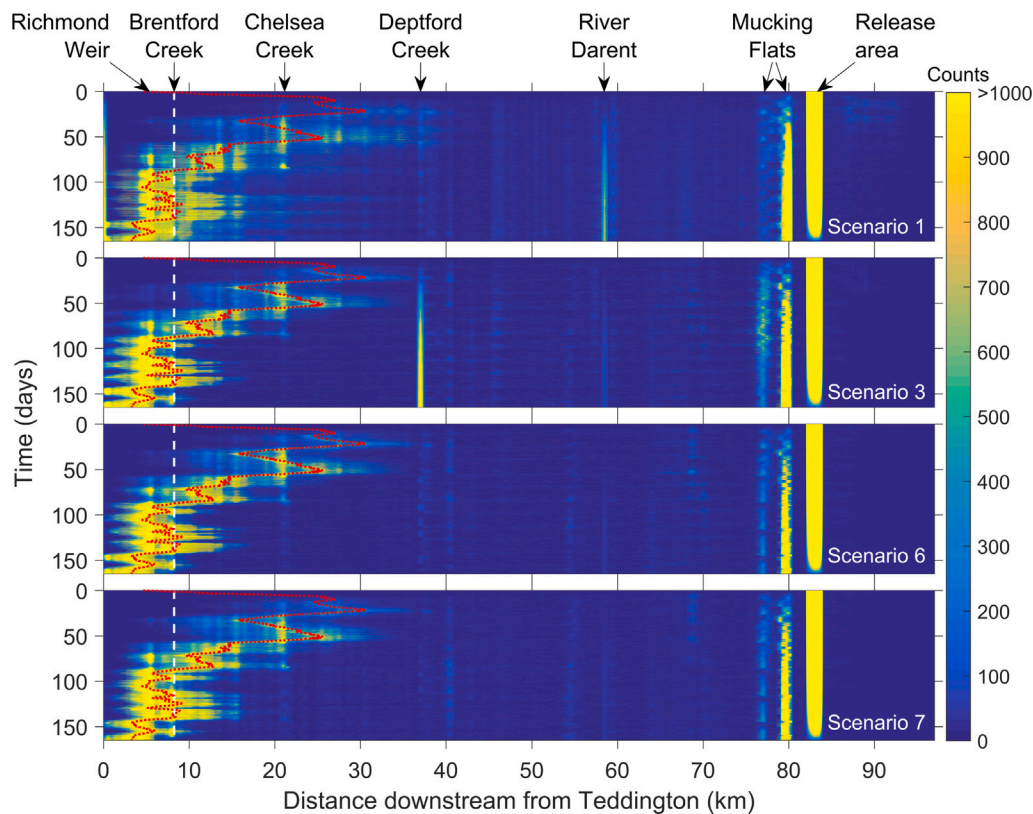
Fig. 5. Spatiotemporal variability in agent density along the channel centreline. Time is downwards along the *y*-axis and distance from Teddington Lock is along the *x*-axis. The colours represent the number of agents counted within 500 m sections along the centreline. Locations along the estuary are labelled at the top and the high water position of the salinity threshold (S_{thresh} = 0.04 ppt) is overlaid for reference (red dashed line).

agents could not easily maintain proximity to the time-varying location of the S_{thresh} contour. In this scenario, there was also some trapping of agents modelled at the entrance to the River Derwent. The agents in other scenarios that included vertical migration (e.g. Scenario 3, 6 and 7) were more tightly arranged around the high tide position of the S_{thresh} contour (red dashed line in Fig. 5) which was calculated by applying a peak-finding algorithm to the time series of the along-estuary distance of the S_{thresh} contour, after first smoothing the series using a fourth-order low pass Butterworth filter with a 3 h cutoff. The modelled aggregation of agents near to the high tide position of the S_{thresh} contour resulted in the more defined peaks in numbers of agents at the entrance to Brentford Creek, especially when the S_{thresh} contour position coincided with the entrance at around high water slack. For Scenario 3, which includes STST behaviour without edging or drifting, there is some trapping of agents in Deptford Creek. Including edging (Scenario 6) results in much less trapping of agents, with very similar results to the full suite of STST behaviours (Scenario 7) in the final subplot in Fig. 5.

3.5.2. Salinity detection threshold calibration

The salinity detection threshold (S_{thresh}) was calibrated using the results from three ABM simulations covering a range of thresholds (0.02, 0.04 and 0.08 ppt). Time series of the number of agents within a distance of 500 m of the entrance to Brentford Creek were extracted from each simulation and plotted with the measured eel trap data for visual comparison (Fig. 6). To allow a clear comparison, the modelled eel numbers were filtered using a 4th order low pass Butterworth filter with a 5 h cut-off frequency so as to remove the tidal signature in the agent numbers. This was due to variability in the number of modelled agents passing the entrance to Brentford Creek at different stages of the tide, thus creating scatter in the time series. Also, the eel trap data were a cumulative measurement of eel numbers over the sample

interval (approximately 24 h), and therefore tidal variability was not present in the data. The modelled eel numbers were also arbitrarily scaled by a factor of 0.2 to allow a visual comparison with the eel trap data (justifiable since absolute eel numbers entering the estuary and the trap efficiency was not known). The timing of the peaks become less comparable to the data using the 0.08 ppt threshold Fig. 6. The results using the 0.02 and 0.04 ppt thresholds are very similar to each other, but a 0.02 ppt threshold shows an early peak occurring in late July which is not in the trap data. A threshold of 0.04 ppt was therefore chosen for the STST sensitivity tests.

3.5.3. Comparison between modelled and measured numbers of eels at Brentford Creek

Comparison of the time series of eel numbers near the entrance to Brentford Creek for all the modelled STST sensitivity tests, shows only small differences between almost all of the scenarios (Fig. 7). The exception is Scenario 1 (constant swimming) which has a more gradual increase in arriving numbers with smaller peaks compared to the other scenarios.

Whilst there are discrepancies in the absolute numbers, the overall trends indicate that the ABM performed well in predicting peak arrival times at Brentford Creek.

Some differences can be seen between the model and observations. For example, there are some small early peaks in modelled eel numbers which are not observed in the data. This might be due to over-simplification in the model. For example, the arrival rate of the eels at the mouth of the Thames in the model is assumed to be constant, whereas in reality there is likely to be a gradual increase in numbers over time followed by a decrease due to the hatching rate of the eel larvae, temperature dependency (as described in Section 3.3) and other variability along their journey from the Sargasso Sea. Small inaccuracies in the modelled salinity might also lead to relatively large
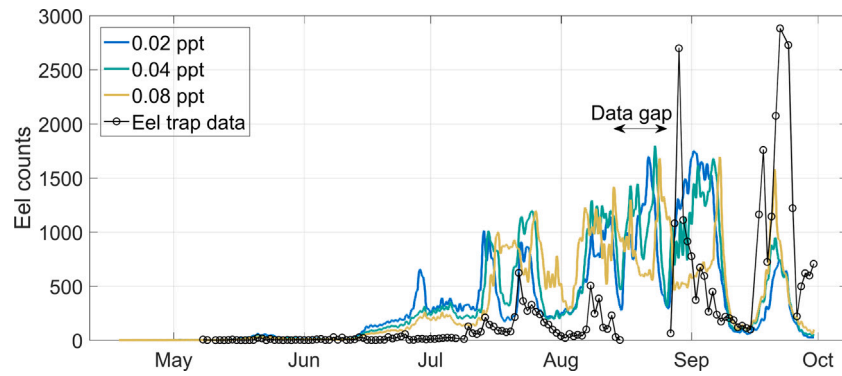
Fig. 6. Sensitivity of salinity detection threshold (S_{thresh}) on the temporal pattern of eel numbers near Brentford Creek for the period May–Oct 2014. Coloured lines denote different salinity thresholds, the black line denotes eel trap data at Stoney Sluice.
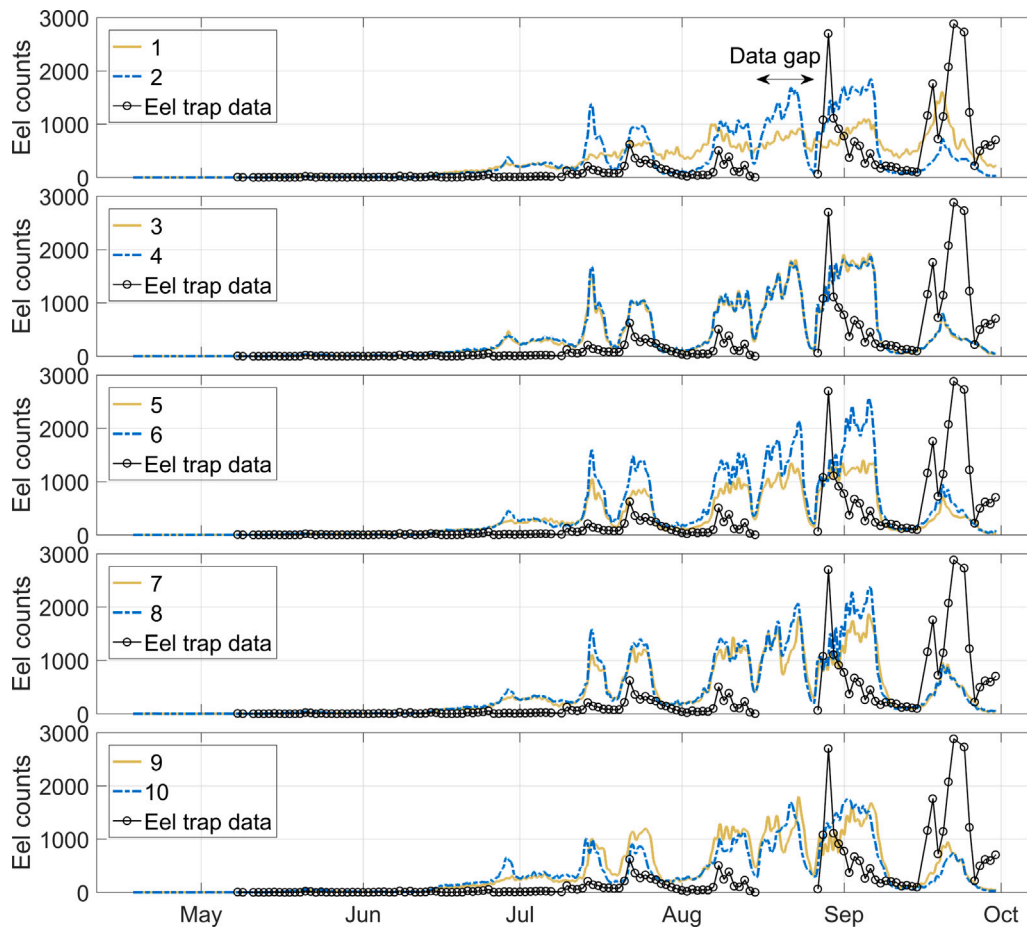

Fig. 7. Comparisons of ten different scenarios (coloured lines) of the ABM with eel trap data (black line) at Brentford Creek. Each colour represents a different scenario (see main text for explanation).

differences since the threshold of salinity detection was found to be a sensitive parameter for controlling the timing of arrival of the eels. The arrival rate is also likely to vary with offshore sea conditions.

The measured peaks in eel numbers tend to rise rapidly followed by a more gradual decrease. The modelled peaks in agent numbers also rise in a similar manner but the numbers tend to remain higher for longer than the data, followed by a rapid decrease. A possible reason for this is that the model does not remove agents during the simulation as they pass Stoney Sluice,

Differences between the model and observations are also expected because the eel trap measurements were made at Stoney Sluice (at the junction with Brent River) which is located about 300 m upstream from

the entrance to Brentford Creek. The modelled agents, on the other hand, were counted in a zone centred on the entrance to the creek (refer to Fig. 4). The agents were counted in this way because the creek entrance was not modelled in high detail and the creek did not extend all the way up to Stoney Sluice (the unmodelled portion of the creek is coloured white in Fig. 4). A future improvement would be to more accurately represent the creek in the model.

Despite all these potential sources of error, the timing of the modelled peaks compare well with the trap data. The time at which eels first start arriving at Brentford Creek and the general increase in numbers over time are also reproduced well in the model.
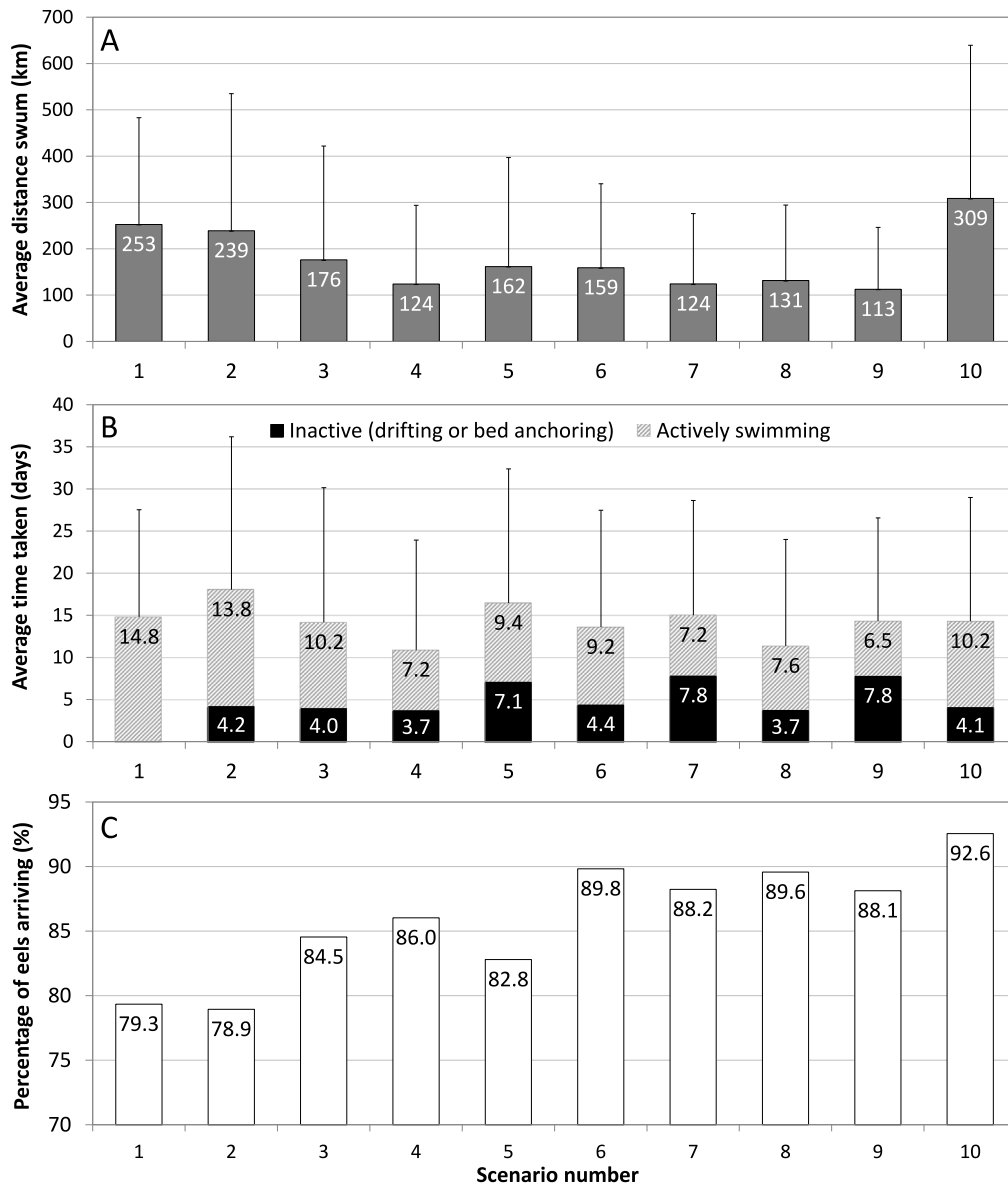
Fig. 8. Results from the ten juvenile eel ABM scenarios (see Table 2) of upstream migration of eels along the Thames Estuary showing: (A) the average through-water distance swum to reach Brentford Creek (+ 1 SD); (B) the average time taken (+ 1 SD), divided into periods of activity (swimming) and inactivity (drifting or bed anchoring), and; (C) the percentage of released agents that have arrived by the end of the simulation. See main text for description of each scenario.

3.5.4. Relative efficiency of STST behaviours

Results from each of the model scenarios for assessing the efficiency of the various STST sub-behaviours are shown in Fig. 8. Fig. 8A and 8B show the average distance swum and migration time (+ SD) to reach Brentford Creek, respectively. The migration time is split according to the amount of time spent being active (i.e. swimming) and inactive (i.e. bed anchoring or drifting). Fig. 8C shows the cumulative percentage of agents, out of the total number of released agents, that reached Brentford Creek by the end of each scenario. The relative energy expenditure (E_{rel}) for each scenario, calculated using Eq. (6) and expressed as percentages, are given in Table 3 (ranked according to minimum energy).

Overall, if daylight avoidance (diel) behaviour was not included, the most energy efficient migration was achieved using just two STST behaviours (ebb tide bed anchoring and upward migration during flood) (Scenario 4). With diel behaviour, a factor likely to improve migration success due to reducing predation, the most energy efficient scenario includes all of the STST behaviours (Scenario 7). The effect

of the different tested behaviours on the model results will now be described in more detail.

Constant swimming: For Scenario 1, which excluded any STST or diel behaviours, the average migration time of 14.8 days was the fifth fastest out of the ten scenarios. However, because the agents spent the whole time actively swimming, including during the fast flowing ebb tide which pushed them back seaward, the average distance swum (253 km) was the furthest out of all the runs with the same swim speed. Consequently it ranked seventh in terms of relative energy expenditure (Table 3). Furthermore, the percentage of released agents that made it to Brentford Creek by the end of the model run (79%) was the second lowest overall.

Diel behaviour: In terms of relative energy expenditure, scenarios that did not include diel behaviour (other than constant swimming) were the most efficient (Scenarios 4, 8 and 9). The most energy efficient upstream migration (Scenario 4) was accomplished simply by implementing both bed anchoring behaviour during the ebb tide (used in all scenarios except number 1) and upward migration during the flood tide (used in all scenarios except numbers 1, 2 and 5). Using just

Table 3

Average modelled eel energy expenditure for estuary migration relative to constant swimming (Scenario 1) expressed as a percentage and ranked according to minimum value.

Rank	Scenario	E_{rel} %
1	4[a]	62
2	8[a]	65
3	9[a]	71
4	7	76
5	6	78
6	3	83
7	5	88
8	1[a]	100
9	2	109
10	10	135

[a] No diel behaviour.

these two behaviours, Scenario 4 resulted in the shortest time taken to reach Brentford Creek (10.9 days) and the equal second shortest distance swum (124 km). It also performed best in terms of energy expenditure (Table 3), using only 62% of the energy compared to constant swimming.

Diel behaviour (i.e. anchoring during daylight) was found to reduce the efficiency of migration by increasing both the time of migration and the average distance swum. This is shown in Fig. 8 by comparing Scenario 3 with 4 and Scenario 7 with 9 . For Scenario 3, the average distance swum was 176 km, reducing to 124 km in Scenario 4 which had diel behaviour switched off. Similarly, the distance swum reduced from 124 to 113 km for Scenarios 7 and 9. In both cases the agents swam less distance and a higher percentage successfully arrived when they did not perform diel behaviour.

Although Scenario 4 performed best overall in terms of energy usage, the most optimal strategy in terms of distance swum was Scenario 9 which included all of the considered behavioural strategies other than diel behaviour. Under this treatment, the average distance swum to reach Brentford Creek was 113 km (lowest overall), the average time taken was 14.3 days (fourth lowest) and 88.1% (second highest) of the released agents arrived successfully (Fig. 8C).

Scenario 2 was the only scenario with standard swim speed that was less efficient than constant swimming (Scenario 1), with a relative energy expenditure of 109%. This is because the energy saving due to ebb tide bed anchoring was not enough to overcome the additional energy expenditure due to diel behaviour (i.e. additional time spent anchoring on the bed). However, by further including upward migration (Scenario 3) a relatively large increase in efficiency was achieved, with the distance swum reducing from 239 km to 176 km and the time of migration reducing from 18 days to 14.2 days. The resultant reduction in energy expenditure (26%) was the largest efficiency saving due to the addition of any single behaviour.

Drifting: Passively drifting rather than swimming during the flood tide (as in Scenarios 5, 7 and 9) reduced the average distance the agents had to swim to reach Brentford Creek, but increased the duration of the migration. This is seen in Fig. 8 by comparing Scenarios 6 and 7 in the which the modelled distance swum reduced from 159 km to 124 km, respectively, whereas the average time taken increased from 13.6 to 15.0 days. The overall effect in terms of energy expenditure (Table 3) was beneficial, but only for scenarios that included diel behaviour. With diel behaviour, the effect of including drifting is shown by comparing Scenario 6 with 7 in which the relative energy expenditure decreased slightly from 78% and 76%, or Scenario 2 with 5 which showed a decrease from 109% to 88%. Without diel behaviour, the effect of drifting is seen by comparing Scenario 8 with 9 in which the relative energy expenditure rose from 65% to 71%.

Edging: Including edging behaviour (Scenarios 6 to 10) had the effect of reducing energy expenditure, but again only for scenarios

that included diel behaviour. Comparing Scenario 3 with 6, which included diel behaviour, the addition of edging behaviour resulted in a slight reduction in average distance swum (176 to 159 km) and a decrease in time taken (14.2 to 13.6 days). This led to a reduction in the relative energy expenditure from 83% to 78% (ranked sixth and fifth in Table 3). In contrast, comparing Scenario 4 and 8 (ranked first and second), which did not include diel behaviour, the addition of edging behaviour resulted in a slight increase in the distance swum (124 to 131 km), time taken (10.9 to 11.3 days) and relative energy expenditure (62 to 65%).

Edging behaviour also led to a marked increase in the percentage of released agents reaching Brentford Creek, rising from 84.5% to 89.8% for Scenario 3 and 6, respectively. A similar increase was modelled between Scenario 4 (86%) and 8 (89.6%). This appears to be due to fewer agents becoming trapped in creeks and on tidal flats (in particular Deptford Creek and Mucking Flats) further downstream (Fig. 5).

Faster swim speed: Scenario 10, which used the same parameters as Scenario 6 but with a faster average swim speed, was by far the least efficient option (135% of the energy expended compared to Scenario 1). The total distance swum was 309 km which was almost double the distance swum for Scenario 6. However, this scenario did result in the largest number of agents arriving at Brentford Creek by the end of the simulation (92.6%).

4. Case study 2: Assessment of juvenile eel entrainment in a power station intake and outfall in Milford Haven Waterway

4.1. Overview

In this case study the developed ABM is used to predict the rate of entrainment of juvenile eels in the cooling water intake and outfall of Pembroke gas-fired power station during their migration up Milford Haven Waterway (MHW) in relation to those successfully reaching any of the rivers adjoining the estuary.

4.2. Site description

The study location is situated in southwest Wales, where the Eastern and Western Cleddeau Rivers merge with the River Carew and Creswell River to form the Daugleddau Estuary (Fig. 2). This drains into the Celtic Sea along with the Pembroke River via the MHW. With a length of approximately 27 km and surface area of 55 km², it is the largest estuary in Wales. It originated as a flooded valley during the last Ice Age, and as a result is one of the deepest natural harbours in the world. Since the 1960s, it has been extensively used for industry, freight and tourism. The cooling water intake to Pembroke gas-fired power station is located in the Pembroke River, close to where it merges with the MHW, whereas the outfall is located in the MHW (Fig. 9).

Although there is currently no commercial eel fishing on the MHW, it is close to the Severn Estuary, which features intensive fisheries (ICES, 2014). It can therefore be hypothesised that juvenile eels are capable of entering the MHW and attempt to progress inland via this estuary. Small numbers of juvenile eels have indeed been recorded as part of the monitoring of impingement of fish on the screens installed on the intakes of the power station. Generally fewer than 10 juvenile eels are found per year, in either January or February (RWE Npower, pers. comm.). However, the 6 mm mesh size of the screens is large enough for juvenile eels to pass through and losses could be considerably higher (Environment Agency, 2015).
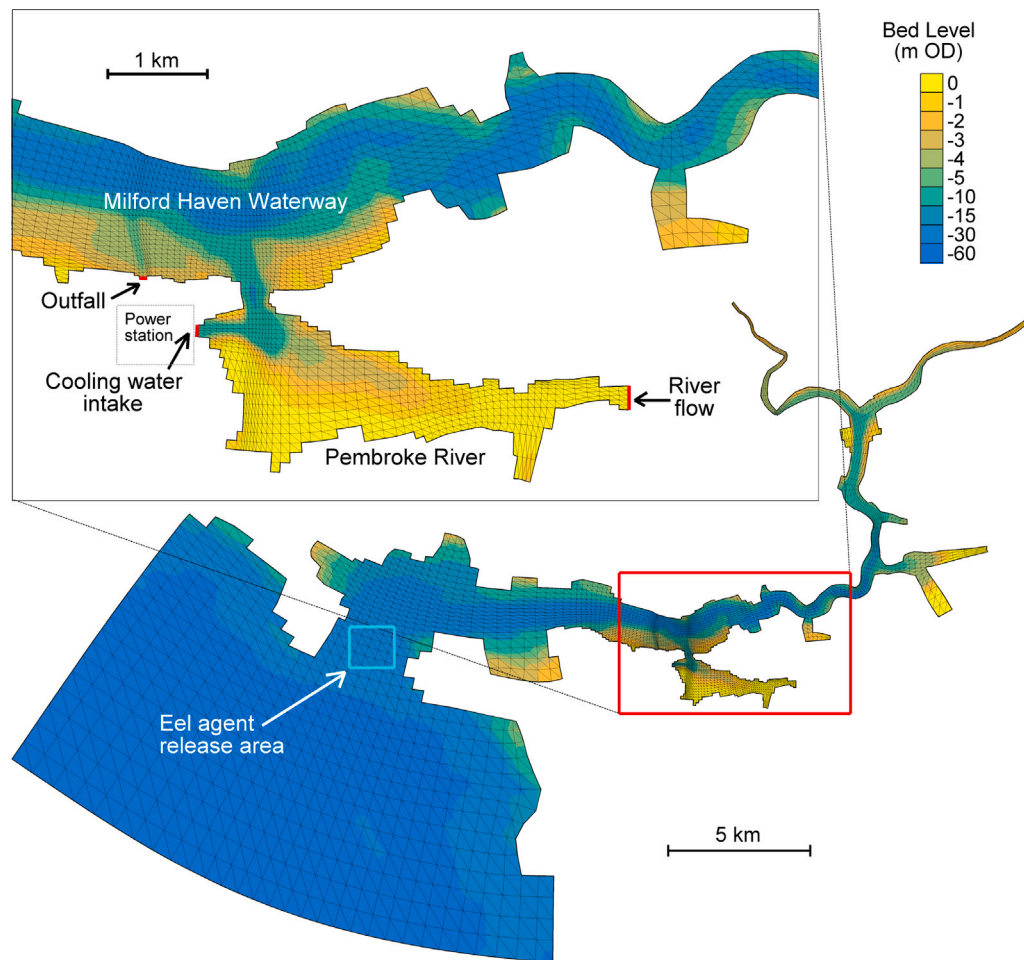
Fig. 9. Milford Haven Waterway model mesh and bathymetry, showing area in which eel agents were released. The zoomed portion shows the locations of the intake and outfall of the gas-fired power station where juvenile eels are potentially entrained.

4.3. Methods

4.3.1. Hydrodynamic model description

A 3D hydrodynamic model of MHW, which included the cooling intake and outfall of Pembroke gas-fired power station, was provided by RWE Npower (Fig. 9). The model, which simulated temperature and salinity as coupled tracers, was developed using the Delft3D modelling suite (https://oss.deltares.nl/web/delft3d). The model mesh consisted of a curvilinear grid made up of 7864 active horizontal cells and 10 planes spaced equally between the bed and the water surface. Resolution of the model varied spatially from 15 m inside the estuary to up to 500 m in offshore regions. The total duration of the simulated flows was 15 days (i.e. a spring–neap cycle).

4.3.2. Power station intake and outfall entrainment assessment

The same parameters as used for Scenario 7 from the Thames Estuary simulations were used (i.e. all STST behaviours and diel behaviour), but now applied to the Milford Haven Waterway. These settings were the most energy efficient out of the tested scenarios that included diel behaviour (Table 3).

Agents were released into the model en masse at the start of the simulation in a rectangular region (1578 x 1442 m) in the mouth of MHW (Fig. 9). The horizontal spacing of the released agents in this areas was 5 m, resulting in a total of 91,324 individuals released, which were then tracked for the 15 day period as they navigated up the estuary.

To assess the probability of entrainment, agents entering the power station intake and outfall at each model time step were counted. To understand the relative impacts on numbers, agents were also counted when they reached either of the rivers that flow into MHW. This was achieved by defining rectangles at the intakes, outfall and each of the tributaries (Fig. 10). Individuals entering the rectangles were assumed to have either been entrained or reached a tributary and were counted according to their location, and then removed from the simulation.

4.4. Results

The cumulative number of modelled agents entering either the power station intake or outfall or successfully reaching each of the adjoining rivers is shown in Fig. 11. Over the 15 day model duration the majority (77.3%) of agents reached one of the rivers.

The predicted number of eels entering the intake and outfall of the power station was 2.0% and 4.7%, respectively. For those that successfully reach a river, the highest percentage of agents reached the Western Cleddau with a total of 22.7% (Table 4). The adjacent Cleddau Ddu received 19.7% of agents. Far fewer tended to swim up the Cresswell and Carew River at 4.6 and 9.0% respectively.

Pembroke River received the second highest percentage of released agents at 22.5%. This is interesting because, to get up the Pembroke, eels need to swim past the entrance of the intake. Since 2% of the release agents entered the intake, equal to 9% of those entering through the confluence of the Pembroke and MHW, it suggests that the intake is suitably located for preventing eels from swimming into it for most of the time. This finding is consistent with the small numbers of juvenile
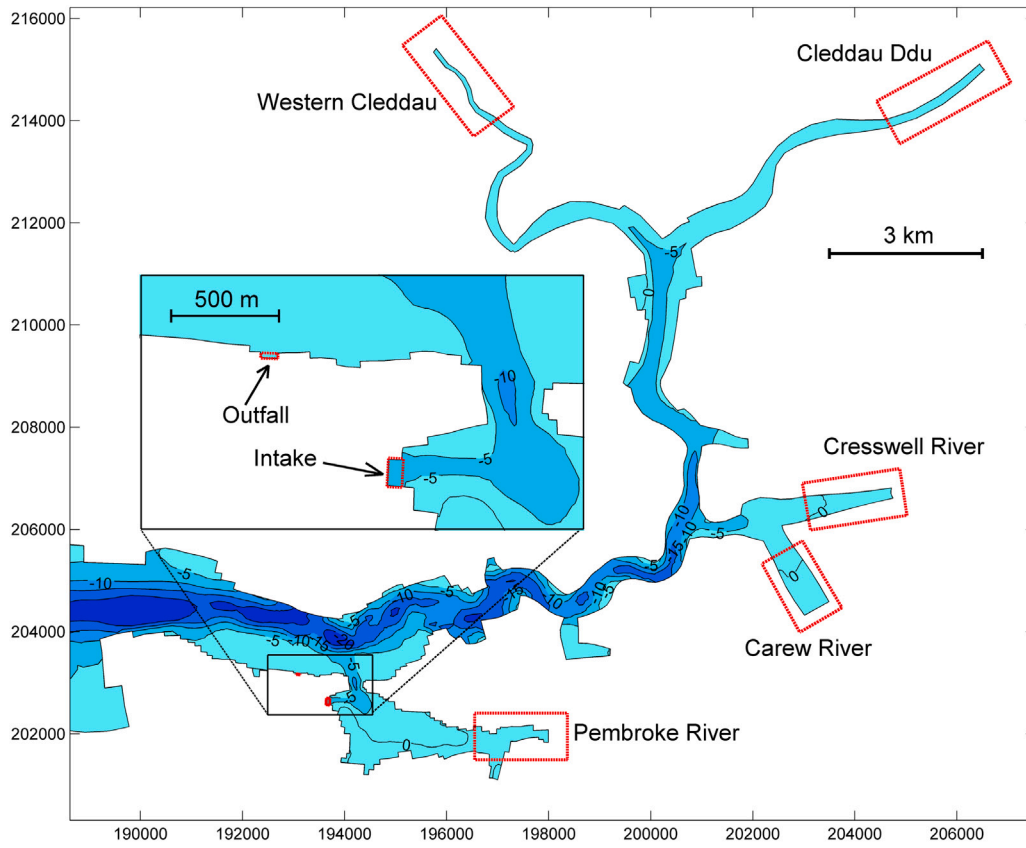
Fig. 10. Locations of power station intake, outfall and tributary polygons used for counting eels reaching various destinations in the simulation. Bathymetry contours are also plotted at 5 m intervals relative to Ordnance Datum Newlyn.
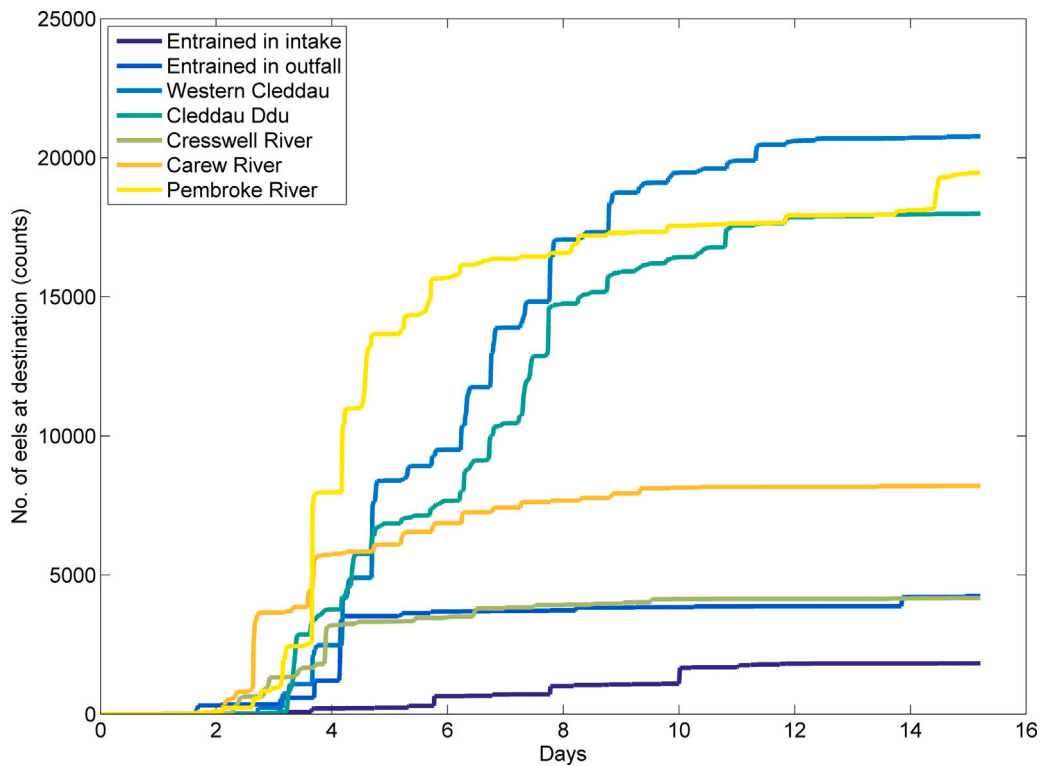

Fig. 11. Cumulative number of modelled eels reaching either the power station intake or one of the rivers over the 15 day period.

Table 4
Number and percentage of eel agents either entrained in the power station intake or reaching a tributary over the 15 day model period (Percentages are relative to total number released).

Destination	Eel agents	
	Counts	%
Power Station Intake	1,829	2.0
Power Station Outfall	4,248	4.7
Western Cleddau	20,769	22.7
Cleddau Ddu	17,989	19.7
Cresswell River	41,74	4.6
Carew River	8,200	9.0
Pembroke River	19,471	21.3
Total	76,680	84.0

eels recorded as being impinged on the intake screens mentioned earlier, although further measurements would be required to substantiate this.

On closer inspection of the model results it was apparent that, at the intake the negative salinity gradient vectors (i.e. towards fresh water) tended to point up the Pembroke River rather than towards the intake. Since the modelled eels preferentially orientated according to this gradient, they generally swam or drifted up the river rather than into the intake. Entrainment occurred for a short period each tide just after low slack water when higher salinity water started to enter the Pembroke. As this water flowed past the entrance to the intake, which still contained relatively low salinity water, the gradient vectors briefly pointed towards the intake (mimicking a flood tide) and the agents drifted into the intake, thus being entrained.

The larger number of agents swimming into the outfall (4.7% of those released) can be explained by the relatively low salinity of the discharged cooling water, compared to the ambient salinity in the MHW, which the eel agents perceived as a river flow. The lower salinity is due to intake drawing water from inside Pembroke River. Interestingly, agents were only able to swim into the outfall when the tide was above approximately mean water level. Below this water level, the shallow depth meant that the flow speed of the outfall discharge exceeded the swim speed of the agents, thus preventing them from entering the outfall. If this had not been the case then it is likely that the numbers entering the outfall would have been significantly higher.

It is noted that a lack of reliable in situ data on eel entrainment at the power station means these modelled entrainment rates cannot yet be confirmed.

5. Discussion

5.1. Key behaviours affecting migration efficiency

Including the selective tidal stream transport (STST) behaviours was found to be essential in reproducing the observed arrival patterns of juvenile eels in the Thames case study. More specifically, the inclusion of downward migration and anchoring at the bed in response to the ebbing tide was found to have the greatest effect on improving the comparison with eel trap data. Scenarios that included downward migration to the bed during the ebb tide and upward migration to the surface at the beginning of each flood tide led to the fastest migration times and shortest average distance swum. This is because the tidal current speeds are fastest at the surface and the vertical distance to reach the surface is relatively small (order of a few metres). The importance of vertical migration and bed anchoring behaviours in response to tidal state is supported by numerous investigations which show that the number of juvenile eel caught using nets in estuaries tends to be higher during the flood tide than during the ebb (Sheldon and McCleave, 1985; McCleave and Kleckner, 1982; Tzeng, 1985; McGovern and McCarthy, 1992; Ciccotti et al., 1995; Arribas et al., 2012).

In terms of relative energy expenditure, a clear distinction was found between scenarios which included diel behaviour and those that did not. Without diel behaviour the energy expenditure was lower. This is understandable since diel behaviour (i.e. bed anchoring during daylight) is for predator avoidance rather than efficiency of movement. The most energy efficient scenario overall did not include diel behaviour and only included bed anchoring during the ebb and upward migration during the flood (Scenario 4). However, with diel behaviour included, the most efficient method was found to be that which included all of the STST behaviours (Scenario 7).

Interestingly, for scenarios that did not include diel behaviour, but included bed anchoring and upward migration, the addition of both edging and drifting behaviours resulted in an increase in energy expenditure. For example, Scenario 9, which included all STST behaviours apart from diel behaviour, only ranked third in terms of energy expenditure, behind Scenario 8 which did not include edging (Table 3). Scenarios that included diel behaviour showed the opposite effect, with energy expenditure reduced if edging or drifting were added.

The effectiveness of edging behaviour by juvenile eels has not been reported on widely elsewhere. During this study, edging was found to reduce the distance swum to reach Brentford Creek. Reasons for this are difficult to determine precisely from the model results, but it is likely to be a combination of several factors. For instance, flows along channel margins are generally slower, thus offer less impedance. The shallower depths also mean that the eels can swim to the bottom for anchoring more quickly when necessary. Keeping to the side of the estuary with the slowest ebb tide flows also has the effect of directing the eels to the inside of meanders, thus leading to a shorter and more optimal route. In the model results, edging behaviour also increased the agents' chances of successfully reaching Brentford Creek. It is unclear exactly why this is the case, but it appeared that the lateral movement helped the agents avoid obstacles such as bridge piers, headlands or embayments along the route. To simulate the edging behaviour, a relatively simple yet effective method was developed and implemented, whereby the eels altered their heading by 45° towards slower water either side of them. Aiming directly towards the channel edges (i.e. adjusting their direction by 90°) was found to be detrimental to their movement because the flow tended to carry them downstream whereas adjusting by 45° towards the lower flow direction meant that half of their swim speed was utilised in swimming against the flow. Since, by definition, the flow speed during edging was less than or equal to their swim speed they then lost relatively little ground.

The active swim speed of the agents was also found to be an important parameter for migration efficiency. Swimming faster was found to reduce the overall efficiency and, perhaps counter-intuitively, did not improve the time of migration. This was because a main limiting factor on the agent progression in this instance was the salinity detection threshold (S_{thresh}) which, due to the low salinity in the estuary between April and June, initially prevented them from navigating directly to Brentford Creek. Hence, although the agents swam faster, they simply reached the freshwater more quickly and then could not navigate further due to the lack of a salinity gradient to follow. The subsequent delay therefore meant they expended more energy.

5.2. The importance of freshwater discharge on navigation

During the modelling of eel migration in the Thames estuary case study, it was found that the detection threshold for salinity was an important calibration parameter. During periods of low river discharge, especially during larger spring tides, the saltwater mixing zone progresses further inland and hence the eels look for sources of freshwater further up the estuary. Seasonal and daily variability in river discharge therefore must play a role in the navigation of eels in estuaries. River discharge is generally not reported as often as other factors, such as temperature, as a cue for eel migration and it can also have an inhibiting effect if the discharge is high enough to lead to fast opposing

flow speeds (Gandolfi et al., 1984; Mouton et al., 2011). River discharge tends to have a gradual effect on the large scale salinity distribution in estuaries as a result of mixing with tidal saline waters (Cresci, 2020). More locally, for example near weirs and sluices, the variability in river discharge will have a more pronounced effect on the salinity and/or odour concentration and therefore will be more important for navigation over shorter time and space scales.

In this modelling study, it has been assumed that the eels directly detect the salinity (or rather the freshness) of the water in order to align themselves for navigation. However, they could alternatively use their olfactory organs to sense some other chemical compound within the water other than salinity. Previous researchers have shown that juvenile eels prefer natural inland surface water over odourless water with the same physical properties (Creutzberg, 1961). Attractive substances include, but are not limited to, earthy and green odours (Sola and Tongiorgi, 1996), amino acids (Sola et al., 1993) and bile salts or taurine which are readily released from other eels (Sola and Tosi, 1993).

Whatever the attractive property of the freshwater, the outcome of modelling is likely to be broadly similar to that presented here. This is because what is being modelled is the mixing of two water bodies distinguished according to the concentration of a conservative dissolved tracer (either salinity or odour). The concentration of a detectable odour would therefore vary spatially in a similar way to the ratio of freshwater to seawater. An exception to this would be if the odour was specific to just one river adjoining an estuary, in which case navigation would be more directed to that river. Another exception would be if the odour was non-conservative (i.e. it decayed over time via chemical reaction or adsorption onto particulate matter) in which case the concentration could decrease more quickly with distance away from the source of input. Further work is required in this area.

5.3. A tool for assessing barriers to eel recruitment

The Milford Haven Waterway test case highlighted how the ABM developed here can potentially be used to assess entrainment or impingement of individuals at power station intakes. This demonstrated how such models could be a useful tool for assisting in the design stage and environmental impact assessment for new power stations and other infrastructure such as tidal turbines. In turn, such tools are valuable in enabling management to identify and mitigate for the adverse effects of human exploitation of waterways on the migratory success and population status of an endangered species that has experienced a strong decline in recruitment in the past decades (ICES, 2017). An example of this would be to rerun the Thames model without Richmond Weir in place to see what impact it had on the salinity and hence migration patterns of the eels.

5.4. Model limitations and future developments

It has been shown in this study that, by using a combination of the local salinity (or odour) gradient and the current velocity field as a navigational cue, modelled agents are able to swim autonomously up-estuary to reach the source of freshwater. However, it is acknowledged that the behavioural rules governing the eel movement are largely based on theory and there is an urgent need for more data from field and laboratory experiments using live animals to provide supporting (or contradictory) evidence for all of the behaviours included in the ABM. Additional behavioural rules, some of which have been suggested in the literature, that would benefit from further supporting data, and which could readily be implemented and tested in the model, are described below.

In terms of navigation, it is assumed in the ABM that the agents are able to simply detect the salinity gradient and flow velocity field at their present location in time and space. Whilst the flow velocity field (and velocity gradients) may be detected using the lateral lines along either side of the eels' bodies (Bleckmann and Zelick, 2009), the method by which juvenile eels detect the salinity or odour gradient might require a behavioural mechanism. One possibility is that the eels assess the change in salinity over time whilst they are anchored on the bed during the ebb tide (Cresci, 2020). This would provide them with a reference frame for assessing the relative directions of the flow and salinity gradients. Since the model already includes bed anchoring behaviour, this detail could be easily incorporated into the ABM. It has been shown that eels can sense the earth's magnetic field (Cresci et al., 2017) which could provide them with a reference frame regardless of whether they were anchored on the bed. This could assist in determining the correct direction of navigation and requires further investigation.

The described model currently only considers a specific stage of eels' migration as they pass through an estuary. The ABM could be extended further to simulate the change in behaviour as the eels reach the river. Currently in the model, when the agents reach freshwater, they are not able to continue migrating since there is no longer a salinity gradient for them to orientate themselves. Additional navigational cues, such as a time-decaying odours are therefore likely to be important for their migration. A physiological characteristic which might also be important for helping the agents transition between saline to freshwater is the recent finding that they have an accurate circatidal rhythm, which allows them to remember the timing of the flood and ebb tides and behave accordingly (Cresci et al., 2017).

There are also possible improvements to be made in the agents' ability to avoid becoming stranded on intertidal areas. In the Thames Estuary case study, significant numbers of modelled agents became stranded on Mucking Flats. This is unlikely to happen in reality because the eels are able to move over sufficiently damp land, which is a behaviour that was not included in the model described here. Other land avoidance mechanisms could also be included to help reduce stranding, such as programming the agents to swim in the direction of the flow when they encounter very shallow water.

A potentially important environmental variable currently not included in the model is turbidity. In waters with high suspended sediment concentrations, such as the Thames Estuary (Baugh et al., 2013), the associated reduction in underwater light due to turbidity is likely to reduce or even remove the requirement for diel behaviour. The model scenario testing carried out in this study suggested that the inclusion of diel behaviour significantly reduced the migration efficiency. Hence, to accurately simulate upstream migration in a particular estuary, the ABM might be improved by including the response of juvenile eels to local underwater light levels caused by both daylight and time varying turbidity. Achieving this would require laboratory measurements on eel behaviour in response to light levels and also a well calibrated 3D suspended sediment model of the estuary.

Including the above factors would make for an interesting continuation of the current work. Other future directions would be to use the ABM to assess climate change and associated effects of multiple factors (e.g. increases in habitat fragmentation, water abstraction rates and water temperature) on eel recruitment (Drouineau et al., 2018). Finally, there are several other species that make use of STST as juveniles (e.g. plaice), and our ABM could be used to assess their upstream migration with adaptations to species specific behavioural rules (Forward and Tankersley, 2001).

CRediT authorship contribution statement

Thomas Benson: Conceptualization, Methodology, Software, Validation, Investigation, Formal analysis, Writing - original draft, Visualization. **Jasper de Bie:** Conceptualization, Methodology, Software, Validation, Formal analysis, Resources, Writing - original draft. **Jennifer Gaskell:** Conceptualization, Methodology, Software, Validation, Writing - review & editing. **Paolo Vezza:** Conceptualization, Methodology,

Resources, Writing - review & editing. **James R. Kerr:** Conceptualization, Methodology, Software, Resources, Writing - review & editing. **Darren Lumbroso:** Conceptualization, Writing - review & editing, Supervision, Project administration. **Markus R. Owen:** Conceptualization, Methodology, Software, Writing - review & editing, Supervision, Project administration. **Paul S. Kemp:** Conceptualization, Methodology, Writing - review & editing, Supervision, Project administration, Funding acquisition.

Declaration of competing interest

The authors declare that they have no known competing financial interests or personal relationships that could have appeared to influence the work reported in this paper.

Acknowledgements

References

Amaral, S.V., Winchell, F.C., McMahon, B.J., Dixon, D.A., 2002. Evaluation of angled bar racks and louvers for guiding silver phase American eels. In: Dixon, D.A. (Ed.), Biology, Management, and Protection of Catadromous Eels. In: American Fisheries Society Symposium, vol. 33, pp. 367–376.

Arai, T., 2014. How have spawning ground investigations of the Japanese eel *Anguilla japonica* contributed to the stock enhancement? Rev. Fish Biol. Fish. 24 (1), 75–88.

Arribas, C., Fernandez-Delgado, C., Oliva-Paterna, F.J., Drake, P., 2012. Oceanic and local environmental conditions as forcing mechanisms of the glass eel recruitment to the southernmost European estuary. Estuar. Coast. Shelf Sci. 107, 46–57.

Baugh, J., Feates, N., Littlewood, M., Spearman, J., 2013. The fine sediment regime of the thames estuary – a clearer understanding. Ocean Coast. Manage. 79, 10–19, Managing Estuarine Sediments.

Benson, T., Rossington, R., Bruintjes, R., 2016. Putting fish in the tank: An Agent-Based Model with flow interaction. In: 23rd TELEMAC User Conference. Paris, France.

Bleckmann, Horst, Zelick, Randy, 2009. Lateral line system of fish. Integrative Zool. 4 (1), 13–25.

Bonabeau, E., 2002. Agent-based modeling: Methods and techniques for simulating human systems. Proc. Natl. Acad. Sci. 99 (suppl 3), 7280–7287.

Bonhommeau, S., Chassot, E., Planque, B., Rivot, E., Knap, A.H., Le Pape, O., 2008. Impact of climate on eel populations of the Northern Hemisphere. Mar. Ecol. Prog. Ser. 373, 71–80.

Briand, C., Beaulaton, L., Baisez, A., 2006. GEMAC: Glass Eel Model to Assess Compliance. Report, Institution d'Aménagement de la Vilaine.

Bru, N., Prouzet, P., Lejeune, M., 2009. Daily and seasonal estimates of the recruitment and biomass of glass eels runs (*Anguilla anguilla*) and exploitation rates in the Adour open estuary (Southwestern France). Aquat. Living Resour. 22 (4), 509–523.

Calles, O., Karlsson, S., Vezza, P., Comoglio, C., Tielman, J., 2013. Success of a low-sloping rack for improving downstream passage of silver eels at a hydroelectric plant. Freshwater Biol. 58 (10), 2168–2179.

Ciccotti, E., Ricci, T., Scardi, M., Fresi, E., Cataudella, S., 1995. Intraseasonal characterization of glass eel migration in the river Tiber - space and time dynamics. J. Fish Biol. 47 (2), 248–255.

Cresci, A., 2020. A comprehensive hypothesis on the migration of European glass eels (*Anguilla anguilla*). Biol. Rev. 95 (5), 1273–1286.

Cresci, A., Paris, C.B., Durif, C.M.F., Shema, S., Bjelland, R.M., Skiftesvik, A.B., Browman, H.I., 2017. Glass eels (*Anguilla anguilla*) have a magnetic compass linked to the tidal cycle. Sci. Adv. 3 (6), e1602007.

Creutzberg, F., 1961. On the orientation of migrating elvers (*Anguilla vulgaris* Turt.) in a tidal area. Netherlands J. Sea Res. 1 (3), 257–338.

Daewel, U., Schrum, C., Gupta, A.K., 2015. The predictive potential of early life stage individual-based models (IBMs): an example for Atlantic cod *Gadus morhua* in the North Sea. Mar. Ecol. Prog. Ser. 354, 199–219.

De Casamajor, M.N., Bru, N., Prouzet, P., 1999. Influence de la luminosité nocturne et de la turbidité sur le comportement vertical de migration de la civelle d'anguille (*Anguilla anguilla* L.) dans l'estuaire de l'Adour. Bull. Fr. Pêche Pisciculture (355), 327–347.

DeAngelis, Donald L., Mooij, Wolf M., 2005. Individual-based modeling of ecological and evolutionary processes. Annu. Rev. Ecol. Evol. Syst. 36 (1), 147–168.

DEFRA, 2010. Eel Management Plans for the United Kingdom: Thames River Basin District. Report, DEFRA.

Dekker, W., 2003. Status of the European eel stock and fisheries. In: Eel Biology. Springer, pp. 237–254.

Drouineau, H., Durif, C., Castonguay, M., Mateo, M., Rochard, E., Verreault, G., Yokouchi, K., Lambert, P., 2018. Freshwater eels: A symbol of the effects of global change. Fish Fish. 19 (5), 903–930.

Environment Agency, 2015. Screening at intakes and outfalls: measures to protect eel. The eel manual – GEHO0411BTQD-E-E.

European Commission, 2007. Establishing measures for the recovery of the stock of the European eel. EC No 1100/2007.

EWCP, 2017. The Thames European Eel Project Report, 2017. Technical Report, Zoological Society of London, pp. 1–22.

Fischer, H.B., List, E.J., Koh, R.C.Y., Imberger, J., Brooks, N.H., 1979. Mixing in Inland and Coastal Waters. Academic Press, New York, p. 483.

Forward, R.B., Tankersley, R.A., 2001. Selective tidal-stream transport of marine animals. Oceanogr. Mar. Biol.: Ann. Rev. 39, 201–213.

Gandolfi, G., Pesaro, M., Tongiorgi, P., 1984. Environmental factors affecting the ascent of elvers, *Anguilla anguilla* (L.), into the Arno River. Oebalia 10, 17–35.

Gascuel, D., 1986. Flow-carried and active swimming migration of the glass eel (*Anguilla anguilla*) in the tidal area of a small estuary on the french atlantic coast. Helgoland Mar. Res. 40, 321–326.

van Ginneken, V., Antonissen, E., Müller, U.K., Booms, R., Eding, E., Verreth, J., van den Thillart, G., 2005. Eel migration to the sargasso: remarkably high swimming efficiency and low energy costs. J. Exp. Biol. 208, 1329–1335.

Gollock, M., Curnick, D., Debney, A., 2011. Recent recruitment trends of juvenile eels of the River Thames. Hydrobiologia 672 (1), 33–37.

Goodwin, R.A., Nestler, J., Anderson, J., Weber, L., Loucks, P., 2006. Forecasting 3-D fish movement behavior using a Eulerian-Lagrangian-Agent Method (ELAM). Ecol. Modell. 192, 197–223.

Grimm, V., Railsback, S.F., 2005. Individual-Based Modelling and Ecology. Princeton University Press, Princeton, NJ.

Harrison, A.J., Walker, A.M., Pinder, A.C., Briand, C., Aprahamian, M.W., 2014. A review of glass eel migratory behaviour, sampling techniques and abundance estimates in estuaries: implications for assessing recruitment, local production and exploitation. Rev. Fish Biol. Fish. 24 (4), 967–983.

Hvidsten, N.A., 1985. Ascent of elvers (*Anguilla anguilla* (L.)) in the Stream Imsa, Norway. Rep. Inst. Freshwater Res. 62, 71–74.

ICES, 2014. Report of the Joint EIFAAC/ICES/GFCM Working Group on Eel. Report, ICES.

ICES, 2017. Report of the Joint EIFAAC/ICES/GFCM Working Group on Eels (WGEEL). Report, ICES.

Jager, H.I., DeAngelis, D.L., 2018. The confluences of ideas leading to, and the flow of ideas emerging from, individual-based modeling of river fishes. Ecol. Modell. 384, 341–352.

Knights, B., 2003. A review of the possible impacts of long-term oceanic and climate changes and fishing mortality on recruitment of anguillid eels of the northern hemisphere. Sci. Total Environ. 310 (1), 237–244.

MacGregor, R., Mathers, A., Thompson, P., Casselman, J.M., Dettmers, J.M., LaPan, S., Pratt, T.C., Allen, B., 2008. Declines of American eel in North America: complexities associated with bi-national management. In: International Governance of Fisheries Ecosystems. American Fisheries Society, pp. 357–381.

McCleave, J.D., 1980. Swimming performance of European eel (*Anguilla anguilla* (L.)) elvers. J. Fish Biol. 16 (4), 445–452.

McCleave, J.D., Kleckner, R.C., 1982. Selective tidal stream transport in the estuarine migration of glass eels of the American eel (*Anguilla rostrata*). J. Conseil 40 (3), 262–271.

McGovern, P., McCarthy, T.K., 1992. Elver migration in the river corrib system, western Ireland. Ir. Fish. Investigations A (Freshwater)(Ireland).

McLane, A., Semeniuk, C., McDermid, G.J., Marceau, D.J., 2011. The role of agent-based models in wildlife ecology and management. Ecol. Modell. 222 (4), 1544–1556.

Monti, P., Leuzzi, G., 2010. Lagrangian models of dispersion in marine environment. Environ. Fluid Mech. 10 (6), 637–656.

Moriarty, C., 1986. Riverine migration of young eels *Anguilla anguilla* (L.). Fish. Res. 4, 43–58.

Mouton, A.M., Stevens, M., Van den Neucker, T., Buysse, D., Coeck, J., 2011. Adjusted barrier management to improve glass eel migration at an estuarine barrier. Mar. Ecol. Prog. Ser. 439, 213–222.

Naismith, I.A., Knights, B., 1988. Migrations of elvers and juvenile European eels, *Anguilla anguilla* L., in the River Thames. J. Fish Biol. 33 (suppl. A), 161–175.

Nikuradse, J., 1933. Stromungsgesetze in Rauhem Rohren (Laws of Turbulent Pipe Flow in Smooth Pipes). VDI-Forschungsheft, Germany, p. 361.

Ospina-Alvarez, A., Catalán, I.A., Bernal, M., Roos, D., Palomera, I., 2015. From egg production to recruits: Connectivity and inter-annual variability in the recruitment patterns of European anchovy in the northwestern Mediterranean. Prog. Oceanogr. 138, 431–447.

Piper, A.T., Manes, C., Siniscalchi, F., Marion, A., Wright, R.M., Kemp, P.S., 2015. Response of seaward-migrating European eel (*Anguilla anguilla*) to manipulated flow fields. Proc. R. Soc. B 282, 20151098.

Prandtl, L., 1925. Bericht uber untersuchungen zur ausgebildete (Report on investigations of developed turbulence). ZAMM 5, 136–139.

Rossington, K., Benson, T., 2020. An agent-based model to predict fish collisions with tidal stream turbines. Renew. Energy 151, 1220–1229.

Russon, I.J., Kemp, P.S., Calles, O., 2010. Response of downstream migrating adult European eels (*Anguilla anguilla*) to bar racks under experimental conditions. Ecol. Freshwater Fish 19 (2), 197–205.

Sheldon, M.R., McCleave, J.D., 1985. Abundance of glass eels of the American eel, *Anguilla rostrata*, in mid-channel and near shore during estuarine migration. Nat. Can. 112 (3), 425–430.

Sola, C., Spampanato, A., Tosi, L., 1993. Behavioural responses of glass eels (*Anguilla anguilla*) towards amino acids. J. Fish Biol. 42 (5), 683–691.

Sola, C., Tongiorgi, P., 1996. The effect of salinity on the chemotaxis of glass eels, *Anguilla anguilla*, to organic earthy and green odorants. Environ. Biol. Fishes 47 (2), 213–218.

Sola, C., Tosi, L., 1993. Bile salts and taurine as chemical stimuli for glass eels, *Anguilla anguilla*: a behavioural study. Environ. Biol. Fish. 37 (2), 197–204.

Soulsby, R.L., 1990. Tidal-current boundary layers. Ocean engineering science, parts A and B. In: The Sea—Ideas and Observations on Progress in the Study of the Sea, Vol. 9. John Wiley and Sons, pp. 523–566.

TELEMAC-MASCARET Consortium, http://www.opentelemac.org. http://www.opentelemac.org.

Tesch, F.W., 2008. The eel. John Wiley & Sons, p. 408.

Tzeng, W.-N., 1985. Immigration timing and activity rhythms of the eel, *Anguilla japonica*, elvers in the estuary of northern Taiwan, with emphasis on environmental influences. Bull. Jpn. Soc. Fish. Oceanogr. 47 (48), 11–28.

Vezza, P., Libardoni, F., Manes, C., Tsuzaki, T., Bertoldi, W., Kemp, P.S., 2020. Rethinking swimming performance tests for bottom-dwelling fish: the case of European glass eel (*Anguilla anguilla*) swimming time. Sci. Rep. 10 (16416) 2045–2322.

Vøllestad, L.A., Jonsson, B., 1988. A 13-year study of the population dynamics and growth of the European eel *Anguilla anguilla* in a Norwegian river: Evidence for density-dependent mortality, and development of a model for predicting yield. J. Anim. Ecol. 57, 983–997.

Vowles, A.S., Don, A.M., Karageorgopoulos, P., Worthington, T.A., Kemp, P.S., 2015. Efficiency of a dual density studded fish pass designed to mitigate for impeded upstream passage of juvenile European eels (*Anguilla anguilla*) at a model Crump weir. Fish. Manage. Ecol. 22 (4), 307–316.

Wallingford, H.R., 2016. Smelt in the Thames: Modelling Report. Technical Report, (DDK2238-RT001-R01-00).

Wallingford, H.R., 2018. Thames Tideway Impacts of DRA (WRMP Option 3): Modelling and analysis of impacts in the Upper Thames Tideway. Technical Report, (DER5714-RT001-R05-00).

White, E.M., Knights, B., 1997a. Dynamics of upstream migration of the European eel, *Anguilla anguilla* (L.), in the Rivers Severn and Avon, England, with special reference to the effects of man-made barriers. Fish. Manage. Ecol. 4, 311–324.

White, E.M., Knights, B., 1997b. Environmental factors affecting migration of the European eel in the Rivers Severn and Avon, England. J. Fish Biol. 50, 1104–1116.